
**INSTITUTO POTOSINO DE INVESTIGACIÓN CIENTÍFICA Y TECNOLÓGICA, A.C.**

**POSGRADO EN CONTROL Y SISTEMAS DINÁMICOS**

# Design of PR protocols for fast consensus in a multi-agent system with real and complex Laplacian eigenvalues

Tesis que presenta

**David Chávez Huerta**

Para obtener el grado de

**Maestro en Control y Sistemas Dinámicos**

Director de la Tesis:

**Dr. Adrián René Ramírez López**

San Luis Potosí, S.L.P., June, 2021


# Constancia de aprobación de la tesis

La tesis **Design of a proportional-retarded controller for fast consensus in a multi-agent system with complex and real Laplacian eigenvalues** presentada para obtener el Grado de de Maestro en Ciencias Aplicadas en la opción Control y Sistemas Dinámicos fue elaborada por (**David Chávez Huerta**) y aprobada el **23 de agosto de 2021** por los suscritos, designados por el Colegio de Profesores de la División de Matemáticas Aplicadas del Instituto Potosino de Investigación Científica y Tecnológica, A.C.

_____

Dr. Arturo Zavala Río
(Presidente)

_____

Dr. Fernando Méndez Barrios
(Secretario)

_____

Dr. Tonámetl Sánchez Ramírez
(Sinodal Suplente)

_____

Dr. Adrián René Ramírez López
(Asesor de la tesis)


# Créditos Institucionales

Esta tesis fue elaborada en la División de Matemáticas Aplicadas del Instituto Potosino de Investigación Científica y Tecnológica, A.C., bajo la dirección del Dr. Adrián René Ramírez López.

Durante la realización del trabajo el autor recibió una beca académica del Consejo Nacional de Ciencia y Tecnología (CVU: 840819) y del Instituto Potosino de Investigación Científica y Tecnológica, A. C.

IPICYT

# Instituto Potosino de Investigación Científica y Tecnológica, A.C.

## Acta de Examen de Grado

El Secretario Académico del Instituto Potosino de Investigación Científica y Tecnológica, A.C., certifica que en el Acta 045 del Libro Primero de Actas de Exámenes de Grado del Programa de Maestría en Control y Sistemas Dinámicos está asentado lo siguiente:

En la ciudad de San Luis Potosí a los 23 días del mes de agosto del año 2021, se reunió a las 11:00 horas en las instalaciones del Instituto Potosino de Investigación Científica y Tecnológica, A.C., el Jurado integrado por:

| | | |
|---|---|---|
| **Dr. Arturo Zavala Río** | **Presidente** | **IPICYT** |
| **Dr. César Fernando Francisco Méndez Barrios** | **Secretario** | **UASLP** |
| **Dr. Adrián René Ramírez López** | **Sinodal** | **IPICYT** |
| **Dr. Tonámetl Sánchez Ramírez** | **Sinodal** | **IPICYT** |

a fin de efectuar el examen, que para obtener el Grado de:

MAESTRO EN CONTROL Y SISTEMAS DINÁMICOS

sustentó el C.

**David Chávez Huerta**

sobre la Tesis intitulada:

***Design of PR protocols for fast consensus in a multi-agent system with real and complex Laplacian eigenvalues***

que se desarrolló bajo la dirección de

**Dr. Adrián René Ramírez López**

El Jurado, después de deliberar, determinó

APROBARLO

Dándose por terminado el acto a las 13:15 horas, procediendo a la firma del Acta los integrantes del Jurado. Dando fe el Secretario Académico del Instituto.

A petición del interesado y para los fines que al mismo convengan, se extiende el presente documento en la ciudad de San Luis Potosí, S.L.P., México, a los 23 días del mes de agosto de 2021.

**Dr. Marcial Bonilla Marín**
Secretario Académico

**Mtra. Ivonne Lizette Cuevas Vélez**
Jefa del Departamento del Posgrado

IPICYT
SECRETARÍA ACADÉMICA
INSTITUTO POTOSINO DE
INVESTIGACIÓN CIENTÍFICA
Y TECNOLÓGICA, A.C.

# Acknowledgments

Firstly, I wish to show gratitude to Dr. Adrian Ramírez for his dedicated support and careful guidance throughout this project. He has been an example of integrity, intellectual honesty and passion for scientific research. This work is better as a result of his direction and I certainly am a better researcher because of it. I want to thank my examiners for their comments on this thesis. Your diligent observations improve this work and are greatly valued.

My gratitude to the many professors that have imprinted their love for art and science with their extraordinary dedication to teaching. I feel particularly indebted to the guidance of Dr. José Espinosa Rosales, Dr. María de Jesús López Toriz, Dr. Oscar Martínez Bravo, Dr. Carlos Hinojosa and Dr. Jesús García Ortíz. I hope to make you proud as I have been proud to be your student. I also acknowledge Alexandra Elbakyan. Without her incredible courage, the work of many young researchers like myself would not be possible. May the dream of open access to science research for every person in the world soon become a reality.

My most sincere gratitude to my parents for their unconditional love, patience and support. To my brothers Moisés and Saúl: I lack the words to describe how much it means to share this work with you.

I thank my friends, for I feel supported by your love and encouragement in every step of the journey: Ana Mendez, Carlos Jano, Eduardo Rodriguez, Farah Ahmed, Hecsari Bello, Hernán Cortez, Jonathan Huerta, Julia Aguirre, Karith Martínez, Levent Chaves, Lissette Tirado, Luis Felipe Cortés, Manuel Martínez, Pablo Fierro, Phebe Bonilla, Sergio Bautista and Valeria Guzman.

To the memory of my uncle Jesús, my friend Salvador and dear Annie. To my dearest Angélica, thank you for your unconditional love and boundless kindness. Finally to Lucky, who kept me in good company for many long hours, made suggestions and double-checked every result on this thesis, to the best of her canine abilities.

# Notation

The symbols $\mu_m$ and $\lambda_m$ will be used to represent the $m$-th real non-zero and the $m$-th complex eigenvalues of the Laplacian matrix $L$, respectively. A complex number $\circ$, will be decomposed as: $\circ = R_\circ + jI_\circ$, where $j$ is the unit imaginary number, and $R_\circ$ and $I_\circ$ representing the real and imaginary components of $\circ$. The symbol $\overline{1,n}$ represents a succession of positive integers up to $n$. $I_n$ will represent an $n$-dimensional square identity matrix, $\mathbb{C}^+$, $\mathbb{C}^-$ and $\mathbb{C}^0$ will represent the right-half, left-half, and imaginary axis on the complex plane. Scalars $|\circ| = (R_\circ^2 + I_\circ^2)^{1/2}$ and $\angle\circ = \arctan(I_\circ/R_\circ)$ are said to be the magnitude and phase of $\circ$, respectively.

# Resumen

Se propone un protocolo de control proporcional-retardado para resolver el problema de consenso en un sistema multiagente con dinámica de integrador único. El enfoque analítico da como resultado reglas de sintonización *listas para usar*. Suponemos que el grafo dirigido que describe la red de agentes es fuertemente conexo. La principal contribución del proyecto radica en que la sintonización está destinada a sistemas con valores propios reales y complejos en la matriz Laplaciana, complementando el estado del arte. El protocolo se demuestra y verifica mediante simulación numérica, así como en la plataforma Robotarium.

# Abstract

A proportional-retarded protocol is proposed to solve the consensus problem in a multiagent system with single integrator dynamics. The analytical approach results in *ready to use* tuning rules. We assume that the directed graph that describes the agents network is strongly connected. The main contribution is that the tuning is intended for systems with real and complex eigenvalues in the network's Laplacian graph, supplementing the current state of the art. The protocol is demonstrated and verified via numerical simulation as well as on the Robotarium platform.

# Contents

# Chapter 1

# Introduction and problem statement

This thesis proposes a proportional-retarded (PR) control protocol to solve the consensus problem in a class of multi-agent systems (MAS) with single integrator dynamic agents. We make extensive use of the theoretical framework developed by Reza Olfati-Saber in his seminal work [18] for analysis of consensus algorithms for multi-agent networked systems. Taking advantage of standard system decomposition techniques, an appropriate factorization of the MAS at hand into individual sub-systems is presented with which Lambert W functions are next incorporated ultimately resulting in analytical tuning formulas for the proposed PR consensus protocol.

We also demonstrate how the aforementioned "ready to use" tuning rules can be conveniently applied in real world problems without further considerations such as additional filtering of measurements. The main contribution of our project is that the proposed tuning technique holds for systems with both real and complex eigenvalues associated with the graph Laplacian of the network. To the best of our knowledge, this has not been previously reported in the open literature and some advancements in this direction are presented only recently in [23, 25] considering either real or complex Laplacian eigenvalues. The effectivity and efficiency of the proposed approach is demonstrated via numerical simulations on various MAS strongly connected directed graphs, and further tested via experiments on Robotarium, a robotic multi-agent testbed developed by Georgia Institute of Technology.

In the rest of this chapter, we present i) a general background pertaining to MAS research, ii) the framework used in this study to analyse MAS's properties and performance and iii) the problem under consideration in this thesis work. Finally, we shall establish the usefulness of our investigation as a completion of the state of the art and list the particular objectives we pursue.

## 1.1 Background

A multi-agent system, or simply MAS, refers to a network of interacting, possible mobile, physical entities that collectively perform a complex task beyond their individual capabilities [6]. In nature, on the one hand, there are many phenomena that may be understood as a MAS. Classical examples are bird flocks, fish schools, bat cauldrons and social insects [8]. In these examples, we may observe collective behavior, e.g. swarming, that emerges based only on local interactions among the members of the group and without any particular supervision of a leader. Considering groups of engineered robotic systems, on the other hand, the last few years have also witnessed multiple efforts to reproduce the collective behavior observed in nature with the aim of rendering these systems with improved features such as robustness, flexibility and resilience [6].

In certain cases, performing a task following a multi-agent-based approach can be more preferable over single-agent-based approaches since in these cases, a MAS may be more flexible and re-organize for the particular needs of the task. For example, a MAS might operate in parallel and would finish the task even if some agents fail, thus improving the overall efficiency and providing reliability. Further, each member of the MAS can be structurally simple and cheap [9]. However, guaranteeing a stable operation of the MAS poses unique challenges as we shall see in detail in this manuscript.

For MAS, the problem of consensus has been extensively studied due to its relevance in a wide variety of fields. In the context of this project, consensus means reaching an agreement in certain quantities of interest that depend on the particular system under consideration. Hence, a consensus protocol may be understood as an interaction rule that specifies how the information is exchanged among the agents and how these agents use the information to ultimately reach an agreement [18]. Even though pioneering research on the *"asynchronous asymptotic agreement problem"* for distributed decision making systems is known since the early eighties [3, 28, 29], it is broadly accepted in the MAS community that the prevailing framework for consensus problems on networked dynamic systems was developed by Olfati-Saber and Murray [19, 18, 20] in 2007. Since then, a broad area of research has been developed in this direction studying various facets of the subject while considering fixed and switching topologies, with or without time delays, for first and second order dynamics, and with the main objective to achieve fast consensus, which is also the focus of this work.

Fast consensus problems in MAS are concerned with having the individual agents reach an agreement as quick as possible. Multiple strategies have been developed to solve this task, some of them, by manipulating certain parameters of the system, tuning the control protocol embedded in the agents and adjusting the communication links between the agents [32, 17, 18].

## 1.2 State of the art

The design of algorithms for fast consensus has received plenty of attention in recent years. An early development was made by Lin Xiao and Stephen Boyd in [32] where the authors described the consensus problem as a linear iteration problem. General conditions on a weighted matrix $W$ associated with the topology of the network were investigated for the system to converge to the average of the state values and guidelines on how to choose $W$ to make the convergence as fast as possible were provided. In [18], Reza Olfati-Saber presented an influential theoretical framework for analysis of consensus algorithms for multi-agent networked systems. There, a broad overview of key results on theory and applications of consensus problems in networked systems were unified in a general framework. Results included basic notions on control theoretic methods for both convergence and performance analysis of distributed consensus protocols. In our project, we heavily rely on this framework.

Several control strategies have also been developed for single integrator MAS subjected to PR consensus protocols. In [14], Min Hyong Koh and Rifat Sipahi take a statistical approach to study fast consensus in a class of MAS with homogeneous delay. There, agents' convergence speed is linked with the topology of the network. Specifically, it is reported that for relatively large delays, consensus can be accelerated up to an order of magnitude reduction in settling time by properly removing some edges in the graph. Even more interesting, by removing the edge that connects the agents with the largest difference between their initial state values, settling time is guaranteed to decrease whenever delay is close to the MAS delay margin. In a latter work [17], Olfati-Saber demonstrated that the algebraic connectivity, i.e. the second smallest eigenvalue of the Laplacian matrix, of a regular network can be considerably increased by a factor of 1000 via random rewiring. This phenomenon, known as *phase transition in algebraic connectivity*, is known to produce the so-called ultrafast consensus in small-world networks.

Supporting the idea that delay can have a positive influence in systems performance, Adrián Ramírez and Rifat Sipahi proposed in [22] a multiple-delay PR protocol to achieve fast consensus in a large-scale MAS. There, the authors demonstrated that the spectral abscissa of the consensus dynamics can be placed at a desired locus provided that the underlying graph is undirected and strongly connected. Considering a single integrator MAS, it is already reported in the literature that a PR consensus protocol can be designed to achieve fast consensus, provided that the Laplacian matrix associated with the network at hand has only real eigenvalues [18, 23]. Likewise, similar results in this research direction have been obtained in the case of complex graph-Laplacian eigenvalues [25]. Based on the above discussions, the main contribution of this project is implementing a PR control protocol that solves the consensus problem as fast as possible when real and complex eigenvalues are present on the graph's Laplacian matrix.

## 1.3 Problem statement

This investigation is focused on reaching fast consensus in a MAS with $n$ single integrators, given by:

$$\dot{x}_i(t) = u_i(t), \quad i = \overline{1,n} \tag{1.1}$$

where $x_i(t)$ is the state of the $i$-th agent and $u_i(t)$ is the corresponding control input. The interconnection pattern among the agents is described by a directed graph $\mathcal{G}$ whose graph Laplacian matrix is allowed to have a mix of real and complex eigenvalues. We adopt the PR consensus protocol:

$$u_i(t) = k_p \sum_{w \in N_i} [x_w(t) - x_i(t)] - k_r \sum_{w \in N_i} [x_w(t-h) - x_i(t-h)], \tag{1.2}$$

where $k_p$ and $k_r$ determine how strong the proportional and retarded control actions shall be and $h > 0$ is an intentional delay induced in agent $i$. Here, the set $N_i$ of neighboring agents connected to $i$ is determined by the directed graph $\mathcal{G}$.

## 1.4 Objectives

As noted before, there is already research on single integrator MAS controlled by PR protocols guaranteeing consensus reaching by carefully selecting particular graphs or by restricting the Laplacian matrix eigenvalues to be real or complex conjugate. In this thesis, we engage in the study of a more general class of system whose Laplacian eigenvalues are allowed to be real and complex, thus complementing the state of the art.

The objective of this project is to develop analytical tuning formulas for the parameters $(h, k_p, k_r)$ that solve the consensus problem for (1.1) controlled by (1.2) as fast as possible based on its dominant roots. In order to achieve this goal, four main tasks are to be completed:

- Factorization of the system. The system is factorized into several independent sub-systems to make the stability analysis tractable.
- Tuning of the PR consensus protocol. A set of tuning rules is proposed to induce convergence “around” the consensus state.
- Stability analysis of the MAS. Using the tuning rules obtained in the previous item, we demonstrate that the proposed tuning is valid for the whole MAS.
- Simulation of the protocol and experimental validation on the Robotarium platform. The consensus protocol is implemented to provide further insight about its performance and limitations.

# Chapter 2

# Preliminaries and problem re-formulation

This chapter briefly summarizes several tools and concepts that are relevant for this thesis. We also restate the problem under consideration in this investigation in terms of the aforementioned concepts while introducing a factorization procedure that facilitates the analysis.

## 2.1 Basic concepts and definitions

In this section, we first review some basic concepts and notions from graph theory. We then introduce the Lambert W function and the spectral abscissa function of a time-delay system.

### 2.1.1 Graph theory

Graph theory has been quite useful to represent MAS and the relation between the properties of the network's graph and certain MAS attributes, such as stability and speed of convergence [18], this much is known is firmly established in the literature. Here, we enumerate several basic concepts of graph theory relevant throughout the project.

The fundamental requirement to study MAS is a way to describe the interactions among the members of the group. To this end, we take from graph theory the notions of vertices —also referred to as nodes— and edges —also known as links—. They can be respectively represented as points in a plane and lines joining the points together, see for instance Figure 2.1. The edges may or may not have a specific direction [2]. When there is no particular direction, a graph denoted by $\mathcal{G}$ may defined by the two sets $X$,$E$ as $\mathcal{G} = (X, E)$ where $X$ and $E$ are the node and edge sets, respectively [2]. It is worthy of mention that $\mathcal{G}$ may be represented in more than in a single way. For example, given

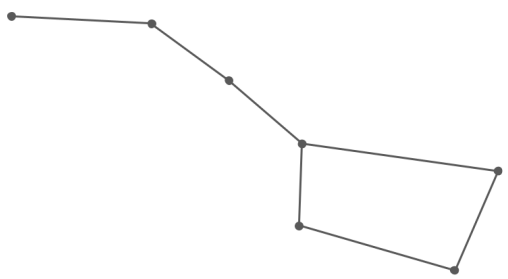

Figure 2.1: A generic representation of a graph where the dots represent the vertices and the straight lines represent the edges.

the sets $X$ and $E$:

$$X = \{x, y, z\} \qquad E = \{a, b, c, d\},$$

any of the representations in Figure 2.2 for $\mathcal{G} = (X, E)$ can be chosen. In other words, the locations of the points and links do not represent any meaningful knowledge. Indeed, the three graphs sketched in Figure 2.2 are isomorphic under a proper labeling of the vertices.

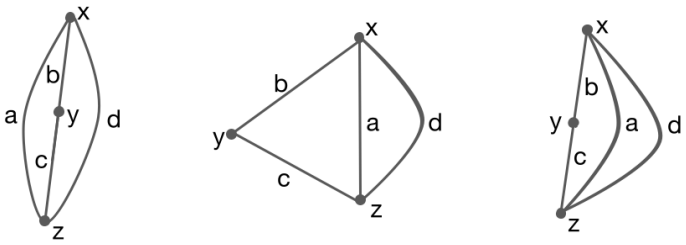


Figure 2.2: Three generic graphs on three vertices.

Two vertices that are joined by an edge are said to be adjacent or neighbors. The degree of a vertex counts the number of its neighbors [16]. When there is a particular direction associated with the edges, it is necessary to represent the edge set $E(\mathcal{G})$ as a subset of the Cartesian product $X \times X$, where $X$ is the vertex set. These objects are called *directed graphs*, or simply *digraph*, and it's common to depict them with arrowheads in the edges, see Figure 2.3.

Having a matrix representation of the graph is fundamental to our project as explained next. The adjacency matrix $\mathcal{A} = [a_{ij}] \in \mathbb{R}^{n \times n}$ provides a straightforward representation of the graph structure. This matrix is such that a non-zero entry $a_{ij}$ indicates the presence of an edge from vertex $j$ to vertex $i$ and a zero entry $a_{ij}$ implies there is no edge connecting these two vertices [2]. To fix the ideas, consider the graph depicted in

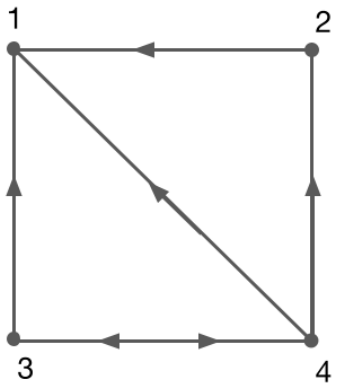


Figure 2.3: A directed graph.

Figure 2.3, its adjacency matrix is:

$$\mathcal{A} = \begin{bmatrix} 0 & 1 & 1 & 1 \\ 0 & 0 & 0 & 1 \\ 0 & 0 & 0 & 1 \\ 0 & 0 & 1 & 0 \end{bmatrix},$$

which contains the same information as that conveyed by Figure 2.3.

Another relevant matrix is the so-called graph Laplacian matrix $L$[1]. For a graph $\mathcal{G}$, the entries of $L$ are defined as [2]:

$$l_{ij} = \begin{cases} \sum_{k=1,k\neq i}^{n} a_{ik}, & j = i \\ -a_{ij}, & j \neq i \end{cases}, \tag{2.1}$$

where $a_{ij}$ is an entry of the adjacency matrix $\mathcal{A}$. For the previous example, the Laplacian matrix is:

$$L = \begin{bmatrix} 3 & -1 & -1 & -1 \\ 0 & 1 & 0 & -1 \\ 0 & 0 & 1 & -1 \\ 0 & 0 & -1 & 1 \end{bmatrix}.$$

Note that every row of $L$ sums zero. Therefore, the Laplacian matrix always has a zero eigenvalue corresponding to the right eigenvector [18]:

$$w_r = (1, 1, ..., 1)^T.$$

Because of this, the rank of $L$ is always less or equal than $n-1$.

[1]The Laplacian matrix can also be defined as $\Delta(\mathcal{G}) - \mathcal{A}(\mathcal{G})$, where $\Delta(\mathcal{G})$ is the in-degree matrix, a diagonal matrix that contains on the $\Delta_{ii}$ entry the number of edges ending on the $i$ vertex.

A directed graph is called strongly connected if and only if any two nodes can be connected by a path defined by the edges. It has been proven that the Laplacian of a strongly connected digraph has an isolated eigenvalue at zero [18]. This will be particularly relevant when using graphs to represent MAS. A spanning tree is a subset of $\mathcal{G}$, which contains all the vertices of $\mathcal{G}$, each pair of them connected by exactly one path. It is known that if a digraph $\mathcal{G}$ can generate a directed spanning tree, all but one Laplacian eigenvalues have positive real parts. However, in directed graphs, the existence of a directed spanning tree is a weaker condition than being strongly connected [26]. This fact will prove useful in what follows.

### 2.1.2 Lambert W functions

In our research, we also use the Lambert W function [5] as means to provide analytical solutions to certain delay difference equations (DDEs). We say that a Lambert W function is any function $W : \mathbb{C} \to \mathbb{C}$ satisfying:

$$W(z)\,\mathrm{e}^{W(z)} = z, \tag{2.2}$$

for all $z \in \mathbb{C}$. The Lambert W function is complex valued and has an infinite number of branches $W_k$, where $k = -\infty, ..., -1, 0, 1, ..., \infty$. The principal branch $W_0$, see Figure 2.4, is significant to the analysis of delayed equations since the system's dominant root $s_0$ can be found with it [33] by using a series expansion or embedded functions in MATLAB®.

We illustrate the use of the Lambert W function with an example from [34] to solve the following scalar system:

$$\begin{aligned} \dot{x}(t) &= ax(t) + a_d x(t-h), \quad t \geq 0 \\ x(t) &= g(t), \qquad\qquad\quad t \in [-h, 0] \end{aligned} \tag{2.3}$$

where $a$ and $a_d$ are scalars, $h$ is the time delay, $x(t)$ represents the instantaneous state of the system, $g(t)$ is the "history" of the system, which may be defined in the space of continuous functions $C([-h, 0], \mathbb{R})$. The solution is given by [1]:

$$x(t) = \sum_{k=-\infty}^{\infty} e^{S_k t} C_k^I, \quad \text{where} \quad S_k = \frac{1}{h} W_k\left(a_d h e^{-ah}\right) + a. \tag{2.4}$$

Here, $W_k$ is the $k$-th root of the Lambert W function and the $C_k^I$ coefficient is determined numerically from the history function. In the next chapter, the principal branch $W_0$ of the Lambert W function becomes relevant to analyze the stability properties of the system. In particular, we emphasize a characteristic of $W_0$ stated in [12].

**Remark 2.1.1.** *For any real number $z \in [-1/\mathrm{e}, \infty)$, the principal branch is a real and increas-*

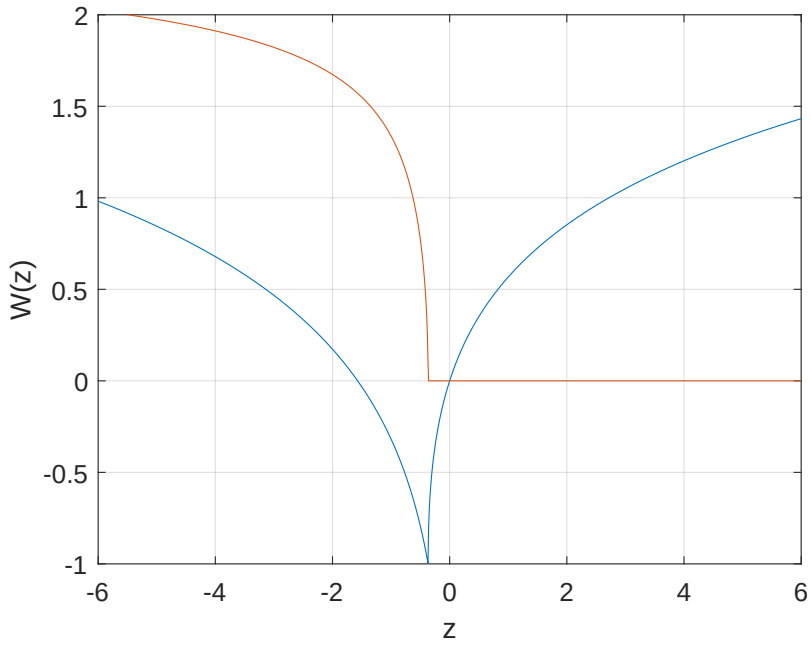


Figure 2.4: The real and imaginary parts of the principal branch $W_0(z)$ are depicted as blue and red solid lines, respectively

*ing function.*

### 2.1.3 The spectral abscissa function

In general, DDEs are infinite dimensional [34]. This infinite dimensionality may lead to an infinite number of characteristic roots. Since the stability of a delayed system may be derived from the location, on the complex plane, of its rightmost characteristic roots, a crucial task is then to determine where such roots are located. With this aim, we next define the spectral abscissa $\alpha$ of a time delay system as in [25]:

$$\alpha = \max\{R_s : s \text{ is a characteristic root of the delayed system, } s \neq 0\}, \tag{2.5}$$

here, $R_s$ is the real part of the characteristic root $s$.

## 2.2 Problem re-formulation

As mentioned in Chapter 1, we aim to analyze system (1.1) controlled by the PR consensus protocol (1.2). Recalling that consensus means to reach an agreement regarding a certain quantity of interest, that may depend on the initial state of all agents.

As in [25], we consider that the PR protocol solves the consensus problem if

$$\lim_{t\to\infty} \|x_v(t) - x_w(t)\| = 0,$$

for all $v, w \in X$. To begin with the re-formulation of the problem, we start by writing the PR controlled MAS in matrix form as:

$$\dot{x}(t) = Ax(t) + Bx(t-h). \tag{2.6}$$

Here, $x$ is the column vector $(x_1 \cdots x_n)^\top$. Additionally, the Laplacian matrix $L$ defined as in (2.1) allows the consensus protocol to be represented by matrices $A$ and $B$ when we define them as $A = -k_p L$ and $B = k_r L$. As described in [15], a substitution of a sample solution of the form $x = \mathrm{e}^{st}\, k$ (here, $k \in \mathbb{C}^{n\times 1}$) in the matrix representation (2.6) generates the system's characteristic function:

$$f(s) = \det(sI - A - \mathrm{e}^{-sh} B). \tag{2.7}$$

Then, the stability properties of (2.6) are given by the distribution of the roots of $f(s)$ on the complex plane $\mathbb{C}$.

Since $L$ has zero row sum, so does $A + B$ [7]. Under the assumption that the graph is strongly connected and that an agent can reach any other agent via a directed path, we have that $A + B$ has only one zero eigenvalue Therefore, the characteristic root at $s = 0$ satisfies (2.7) for any delay $h$. This zero eigenvalue corresponds to the eigenvector $\vec{1} = (1, ..., 1)^T$ and an equilibrium of system (2.6) is a state in the form $x = (x^*, ..., x^*) = x^*\vec{1}$ where all nodes agree on a $x^*$ value, signifying the consensus nature of the PR-controlled MAS [18]. For the remainder of this dissertation, the characteristic root at $s = 0$ will be ignored and stability will be studied around its consensus state, independent of $h$.

**Remark 2.2.1.** *The closed-loop dynamics (1.1)-(1.2), is stable around the consensus state if its spectral abscissa* $\alpha$ *defined in* (2.5) *is strictly negative. Otherwise, the system is unstable and consensus cannot be achieved.*

It is worth mentioning that the stability conditions, as described in the above remark, would not guarantee performance[2] for the closed-loop dynamics. To investigate how fast the agents reach consensus we employ the concept of $\gamma$-stability that will prove to be directly associated with the time of consensus reaching. The dynamics is said to be $\gamma$-stable when $\alpha = -\gamma$ , for a possitive real value of $\gamma$. In the literature, $\gamma$ has been related to the exponential decay rate of the agents' states. This relation is given by the next theorem, taken from [10]:

[2]Remark 2.4.1 is not specific regarding how long will the system take to settle in the consensus state. We consider performance to be directly related with minimizing this settling time.

**Theorem 2.2.1.** *Consider the delayed scalar system:*

$$\dot{x}(t) = ax(t) + ax(t-h),$$

*suppose* $\alpha_o = \max\{R_s : s \text{ is a characteristic root}\}$ *and* $x(\phi,t)$ *is the solution of the delayed scalar system, which coincides with* $\phi$ *on* $[-h,0]$*. Then, for any* $\alpha > \alpha_o$ *, there is a constant* $K = K(\alpha) \geq 1$ *such that:*

$$\|x(\phi,t)\| \leq K\,\mathrm{e}^{\alpha t}\,\|\phi\|_h, \quad t \geq 0, \quad \textit{where} \quad \|\phi\|_h = \sup_{-r\leq\theta\leq 0} \|\phi(\theta)\|.$$

*In particular, if* $\alpha_o < 0$*, then one can choose* $\alpha_o < \alpha < 0$ *to obtain the fact that all solutions approach zero exponentially as* $t \to \infty$*.*

In what follows, we shall show how this result is pertinent to our case. For now, it allows us to state the main objective of this thesis, namely, solve the consensus problem as fast as possible, in a more formal way as the following problem:

**Problem 2.2.1.** *Find analytical formulae to tune* $(h, k_p, k_r)$ *that create the maximum exponential decay rate for* $\gamma$ *based on the dominant roots of system (1.1) controlled by (1.2).*

### 2.2.1 Factorization property

A change of variable facilitates $\gamma$-stability analysis. Introducing $s \to (s-\gamma)$ on (2.7), the real part of the characteristic roots is shifted by $\gamma$. The shifted characteristic function reads:

$$f(\gamma, s) = \det\left(sI_n - \gamma I_n - A - B\,\mathrm{e}^{\gamma h}\,\mathrm{e}^{-sh}\right). \tag{2.8}$$

In this sense, analyzing the stability transitions[3] of (2.8) along the imaginary axis $s = j\omega$ is equivalent to analyzing $\gamma$-stability transitions of (2.7) along the shifted imaginary axis $s = j\omega - \gamma$. In other words, stability of (2.8) implies the $\gamma$-stability of (2.7). The shifted characteristic equation still poses challenges related to its infinite number of characteristic roots and growing complexity, e.g. the number of agents is directly related to the size of the matrices involved. Hence, a decomposition (2.8) is necessary to simplify the task.

Based on standard decomposition techniques [4], we next perform a factorization of the shifted characteristic equation (2.8) where the resulting factors are associated with a finite set of systems with reduced complexity. We shall show how these factors are associated with a specific Laplacian eigenvalue. To this end, let us number and classify the eigenvalues of the Laplacian matrix. Since we assumed a strongly connected digraph and no looped edges that go back to the same vertex. This generates an associated

[3] Using a continuity argument, a characteristic root can migrate from left (right) to right (left) on the complex plane only through the imaginary axis. In particular, a transition from stability to instability happens if the root crossing from left to right of the imaginary axis corresponds to the rightmost root of the system at hand.

Laplacian matrix $L$ with zero row-sum. As discussed before, this results in a single zero eigenvalue for $L$, which is associated with the consensus state. For connected edges $a_{uw} > 0$ and $u \neq w$, the remaining Laplacian eigenvalues have positive real parts provided that the digraph $\mathcal{G}$ has a directed spanning tree.

Given that the literature contemplates the case of only real or only complex eigenvalues, to our best knowledge, here we aim to account for the mixed case, and group them into a set $\rho = (\nu, \mu, \lambda)$ where:

$$\nu = 0 \qquad \mu = (\mu_1, \ldots, \mu_{n_1}) \qquad \lambda = (\lambda_1, \ldots \lambda_{n_2}), . \tag{2.9}$$

Here, the numbering of the eigenvalues is based on their real parts sorted increasingly. Further, for a complex conjugate pair $(\lambda_q, \lambda_{q+1})$, we have $I_{\lambda_q} > 0$. In other words, within a pair of complex conjugate eigenvalues, the element with positive imaginary part goes first. In case $R_{\lambda_p} = R_{\lambda_q}$ for two different pairs, then the numbering respects $I_{\lambda_p} < I_{\lambda_q}$.

**Remark 2.2.2.** *Notice that the elements of a given tuple are not elements of the others and therefore* $1 + n_1 + n_2 = n$. *In brief we can consider* $\rho = (\nu, \mu, \lambda)$ *as an* $n$*-tuple composed of a* $1$*-tuple, an* $n_1$*-tuple and an* $n_2$*-tuple.*

Assuming that the shifted characteristic function $f(\gamma, s)$ can indeed be factorized, let us consider a general class of factors, namely:

$$f_\rho = (f_{\rho_1}, \ldots, f_{\rho_n}), \tag{2.10}$$

where each element is associated with one Laplacian eigenvalue. Then, the following theorem holds.

**Theorem 2.2.2.** *The shifted characteristic function* $f(\gamma, s)$ *in (2.8) satisfies*

$$f(\gamma, s) = \prod_{m=1}^{n} f_{\rho_m}(\gamma, s), \tag{2.11}$$

*where the characteristic factor* $f_{\rho_m}(s, \gamma)$ *is given by*

$$f_{\rho_m}(\gamma, s) = s - \gamma + \rho_m k_p - \rho_m k_r \, \mathrm{e}^{\gamma h} \, \mathrm{e}^{-sh}, \tag{2.12}$$

*and* $\rho_m \in \mathbb{C}^0 \cup \mathbb{C}^+$ *is an eigenvalue of the Laplacian matrix* $L$.

*Proof.* Define the vectors with exponential elements $y(\gamma, t) = \mathrm{e}^{\gamma t} x(t)$ and $y(\gamma, t-h) = \mathrm{e}^{\gamma(t-h)} x(t-h)$. Then, differentiating $y(\gamma, t)$ with respect to time and using these vectors in the matrix representation (2.6) yields:

$$\dot{y}(\gamma, t) = (\gamma I_n + A) y(\gamma, t) + B e^{\gamma h} y(\gamma, t-h). \tag{2.13}$$

Computing the characteristic function for this system we find it to match (2.8). Crucial for this decomposition, the Schur's theorem [11] guarantees the existence of a unitary matrix $U \in \mathbb{R}^{n\times n}$, such that $L = UTU^H$ holds for the Laplacian matrix $L$, where $T$ is an upper triangular matrix whose diagonal entries are the eigenvalues of $L$ and $U^H$ is the conjugate transpose of $U$. Under this unitary transformation, and recalling that $A = -k_pL$ and $B = k_rL$, we introduce the change of coordinates $y(\gamma,t) = U\xi(\gamma,t)$, which transforms system (2.13) into:

$$\dot{\xi}(\gamma,t) = (\gamma I_n - k_pT)\xi(\gamma,t) + k_rT\,\mathrm{e}^{\gamma h}\,\xi(\gamma,t-h). \tag{2.14}$$

The fact that the coefficient matrices in (2.14) are upper triangular implies that the stability of system (2.13) can be studied through $n$ equations with dynamics:

$$\dot{\xi}_{\rho_m}(\gamma,t) = (\gamma - \rho_m k_p)\xi_m(\gamma,t) + \rho_m k_r\,\mathrm{e}^{\gamma h}\,\xi_m(\gamma,t-h), \quad m = \overline{1,n}. \tag{2.15}$$

The characteristic equation of (2.15) is (2.12), which is a factor of $f(\gamma,s)$ in (2.11). This fully justifies our assumption about a general class of factors indicated in (2.10). □

Since we already defined the tuple $\rho = (\nu,\mu,\lambda)$, the characteristic factors can be placed into one of three different classes given by the tuples $f_\rho = (f_\nu, f_\mu, f_\lambda)$, where

$$f_\nu = f_{\nu_1} \qquad f_\mu = (f_{\mu_1},\ldots,f_{\mu_{n_1}}) \qquad f_\lambda = (f_{\lambda_1},\ldots f_{\lambda_{n_2}}), \tag{2.16}$$

whose elements are defined as in (2.12) with $\rho_m \in (\nu,\mu,\lambda)$. From Theorem 2.2.2, it is clear that the elements of the above defined tuples are the characteristic factors of the decoupled subsystems in (2.15). It is worthy of mention that using the tuples description on (2.16), we have that (2.11) can be written in a more concise way as

$$f(s,\gamma) = f_{\nu_1} \times f_{\mathbb{R}} \times f_{\mathbb{C}}, \tag{2.17}$$

where $f_{\nu_1} = s$ is associated with the zero eigenvalue and corresponds to the consensus state of the network. On the other hand, the factors of the products $f_{\mathbb{R}} = f_{\mu_1} \times \cdots \times f_{\mu_{n_1}}$ and $f_{\mathbb{C}} = f_{\lambda_1} \times \cdots \times f_{\lambda_{n_2}}$ are quasipolynomials with respectively pure real and complex coefficients.

### 2.2.2 Spectral abscissas of the characteristic factors

The shifted characteristic function $f(s,\gamma)$ we are concerned with is now decomposed into three main factors $f_{\nu_1}$, $f_{\mathbb{R}}$ and $f_{\mathbb{C}}$. At the same time, these three factors are products of characteristic functions related to individual eigenvalues. Our next result associates the stability of the entire system with the individual spectral abscissas of the tuples $(f_\nu, f_\mu, f_\lambda)$

**Corollary 2.2.1.** *Let $\alpha_{\rho_m}$ be the spectral abscissa of the $m$*th *system*

$$\dot{\zeta}_{\rho_m}(t) = -\rho_m k_p \zeta_m(t) + \rho_m k_r \zeta_m(t-h), \quad m = \overline{2,n}. \tag{2.18}$$

*Then, if $\alpha_{\rho_m} < 0$, system (2.6) is exponentially stable around the consensus state of the network.*

*Proof.* Note that (2.6) and (2.13) are equivalent with $\gamma = 0$. Since $\dot{\zeta}_{\rho_m}(t) \equiv \dot{\xi}_{\rho_m}(0,t)$, it follows that (2.6) is exponentially stable if the spectral abscissas $\alpha_{\rho_m}$ associated with $\dot{\zeta}_{\rho_m}(t)$, $m = \overline{1,n}$, are strictly negative. Equivalently,

$$\alpha = \max_{1 \leq m \leq n} \{\alpha_{\rho_m}\} < 0.$$

On account of $\rho_1 = \nu = 0$, the case $m = 1$ can be ignored in the stability analysis. The proof is completed by noticing that $\alpha_{\rho_m} < 0, m = \overline{2,n}$ ensures $\alpha < 0$. □

We must stress the importance of Corollary 2.2.1 since it guarantees that separately analyzing the $\gamma$-stability of the individual subsystems in (2.18) is equivalent to analyzing the $\gamma$-stability of the complete system (2.6). Keeping the symmetry of the presentation, we let these subsystems form the $n$-tuple $\dot{\zeta}_\rho = (\dot{\zeta}_\nu, \dot{\zeta}_\mu, \dot{\zeta}_\lambda)$, where

$$\dot{\zeta}_\nu = \dot{\zeta}_{\nu_1} \quad \dot{\zeta}_\mu = (\dot{\zeta}_{\mu_1}, \ldots, \dot{\zeta}_{\mu_{n_1}}) \quad \dot{\zeta}_\lambda = (\dot{\zeta}_{\lambda_1}, \ldots, \dot{\zeta}_{\lambda_{n_2}}), \tag{2.19}$$

whose elements come from (2.18) with $\rho_m \in (\nu, \mu, \lambda)$. Since each system depends on a unique Laplacian eigenvalue, we may now define the spectral abscissas $\alpha_\rho = (\alpha_\nu, \alpha_\mu, \alpha_\lambda)$, each one associated with a particular member of $\dot{\zeta}_\rho$, where

$$\alpha_\nu = 0 \quad \alpha_\mu = (\alpha_{\mu_1}, \ldots, \alpha_{\mu_{n_1}}) \quad \alpha_\lambda = (\alpha_{\lambda_1}, \ldots, \alpha_{\lambda_{n_2}}). \tag{2.20}$$

As we have established before, $\alpha_\nu = 0$ can be ignored in the stability analysis. Thus, for $\gamma > 0$, if:

$$\alpha = \max(\alpha_\mu, \alpha_\lambda) < -\gamma, \tag{2.21}$$

then, the whole MAS (2.6) is $\gamma$-stable. Central to our project is to ensure the inequality stated in (2.21) holds. Let us now define the sets:

$$G_\mu = \{g_{\mu_1}, \ldots, g_{\mu_{n_1}}\}, \quad \text{and} \quad G_\lambda = \{g_{\lambda_1}, \ldots, g_{\lambda_{n_2}}\}, \tag{2.22}$$

where $g_{\mu_{m_1}} = (\dot{\zeta}_{\mu_{m_1}}, \alpha_{\mu_{m_1}}, f_{\mu_{m_1}})$ and $g_{\lambda_{m_2}} = (\dot{\zeta}_{\lambda_{m_2}}, \alpha_{\lambda_{m_2}}, f_{\lambda_{m_2}})$. Then, every single element of the $G$ sets consist of a $\dot{\zeta}_\diamond(t)$ system, its corresponding spectral abscissa $\alpha_\diamond$ and characteristic factor $f_\diamond$.

**Definition 2.2.1.** *The set $G_\diamond$ is said to be $\gamma$-stable if one of the following assertions hold:*

*a) The systems in $\dot{\zeta}_\diamond$ are $\gamma$-stable.*

*b) The spectral abscissas in $\alpha_\diamond$ are smaller or equal to $-\gamma$.*

*c) The real part of the rightmost-root of the factors in $f_\diamond$ are smaller or equal to $-\gamma$,*

*where $\diamond$ stands for either a $\mu$ or a $\lambda$ eigenvalue.*

It is worthy of mention that Definition 2.2.1 above states that the stability of $G_\diamond$ implies the stability of the subsystems within the set. Conversely, the stability of the subsystems constituting $G_\diamond$ implies the stability of the set. The reader is referred to [27, p. 315], and the references therein, for a different definition of stability of a set. In what follows, based on the above stated stability notion, we focus on finding conditions for the $G_\diamond$ sets to be stable in the sense of Definition 2.2.1 and based on the location of the rightmost roots of the subsystems.

# Chapter 3

# Fast consensus in MAS

In this chapter, the factorization proposed in Chapter 2 is used to investigate the stability properties of $G_\lambda$, the set associated with complex Laplacian eigenvalues, in the sense of Definition 2.2.1. In particular, we obtain a tuning technique based on the work presented at [23, 25] that guarantees a stable placement of the system's rightmost roots. It is worthy of mention that the approach initially guarantees the $\gamma$-stability of the $G_\lambda$ set. The formulas, however, are also used in $G_\mu$, the set associated with real Laplacian eigenvalues, likewise, $\gamma$-stability in $G_\mu$ is guaranteed as further clarified below. With this aim, both sets are contrasted against each other to determine which sub-system dominates the overall MAS, ultimately resulting in a "re-design" of the parameters of the consensus protocol, required in some particular cases.

## 3.1 Stability of the $G_\lambda$ set

In this chapter we obtain tuning formulas for the parameters of the PR controller with which $\gamma$-stability of the $G_\lambda$ set is guaranteed. First, we present a methodology to place the largest spectral abscissa within $G_\lambda$ at any arbitrary position $\gamma_d$ on the complex plane. Then, we investigate how the $G_\mu$ set behaves under the aforementioned tuning rule. In particular, we study how the stability of the set is affected.

Recall that the subsystems in $G_\lambda$ depend only on complex conjugate Laplacian eigenvalues. Such case is already reported in the literature. Here, we shall use the analysis developed in Ramirez [25], adapted to the problem at hand. Our first objective is to move the characteristic roots of a generic factor $f_{\lambda_q}$ as deep as possible into the left-half complex plane using the shift $\gamma$. To do so, a maximum value for $\gamma$ associated with the $q$-th factor $f_{\lambda_q}$, namely $\bar{\gamma}_q$, is to be found in terms of the proportional constant $k_p > 0$ and further associated with the design parameters in the $(h, k_r)$ domain. We consider

that $f_{\lambda_q}$ implicitly depends on four variables and we search for the maximum value of $\gamma$ such that the $q$-th factor satisfies

$$f_{\lambda_q}(\gamma, j\omega) = 0, \tag{3.1}$$

where $f_{\lambda_q}$ is taken from (2.12) with $\rho_m = \lambda_q$ and $s = j\omega$. Using a continuity argument[1], we have that any pair $(h, k_r)$ satisfying (3.1) generates a characteristic root $s = j\omega - \gamma$ for the non-shifted characteristic equation. Our objectives here are threefold:

*i)* To find an analytical expression for the maximum $\bar{\gamma}_q$ associated with (3.1).

*ii)* To determine whether the characteristic root $s = -\bar{\gamma}_q + j\omega$ indeed corresponds to the spectral abscissa of the system (2.18).

*iii)* To verify that the PR controller design based on the parameters of one factor do not undesirably affect any other factor.

### 3.1.1 Local maxima of exponential decay rates

Let $k_p > 0$, it is clear that the $q$-th factor in (3.1) cannot be solved for $\gamma$ as a function of the known parameters since it implicitly depends on $\omega$, $h$, and $k_r$. Consequently, a maximum for $\gamma$ cannot be explicitly expressed in terms of our design parameters $(h, k_r)$ for a given frequency $\omega$. However, following [24], we have the next theorem characterizing the extrema points of $\gamma$ in $(h, k_r)$ domain:

**Theorem 3.1.1.** *Let $k_p \in \mathbb{R}^+$ and $\lambda_q = |\lambda_q| e^{j\angle\lambda_q} \in \mathbb{C}^+$ with $|\lambda_q| > 0$ and $\angle\lambda_q \in (-\pi/2, \pi/2)$ be given [2]. Then, the spectral abscissa function $\gamma$ exhibits a local maximum in the $(h, k_r)$ domain at:*

$$\gamma_q^i = k_p(R_{\lambda_q} - I_{\lambda_q}/\chi_q^i). \quad i = 1, 2, \ldots, \tag{3.2}$$

*where $\chi_q^i = \text{sign}(I_{\lambda_q})(|\angle\lambda_q| - i\pi)$, subject to:*

$$(h, k_r) = \left( \frac{1}{\gamma_q^i - k_p R_{\lambda_q}}, \frac{-e^{-\gamma_q^i h}}{|\lambda_q| h \cos(-i\pi)} \right). \tag{3.3}$$

*Proof.* Assume that $\gamma$ exhibits a maximum, then $(f_q, \partial f_q/\partial\omega) = (0, 0)$ must be satisfied.

[1] The continuity properties of the eigenvalues of a system with respect to its parameters indicate that a transition from $\gamma$-stability to $\gamma$-instability can only occur if the spectral abscissa crosses the shifted imaginary axis $j\omega - \gamma$, see [15].

[2] Since we are assuming $\mathcal{G}$ has a directed spanning tree, we restrict $\lambda$ to the right-half complex plane.

Collecting the real and the imaginary parts of the above condition yields:

$$k_r \, \mathrm{e}^{\gamma h} \, |\lambda_q| \, \begin{pmatrix} \cos\left(h\omega - \angle\lambda_q\right) \\ \sin\left(h\omega - \angle\lambda_q\right) \end{pmatrix} = \begin{pmatrix} k_p R_{\lambda_q} - \gamma \\ -k_p I_{\lambda_q} - \omega \end{pmatrix}, \tag{3.4}$$

$$h k_r \, \mathrm{e}^{\gamma h} \, |\lambda_q| \, \begin{pmatrix} \sin\left(h\omega - \angle\lambda_q\right) \\ \cos\left(h\omega - \angle\lambda_q\right) \end{pmatrix} = \begin{pmatrix} 0 \\ -1 \end{pmatrix}. \tag{3.5}$$

Eliminating $h$ and $k_r$ from (3.4) and (3.5) leads to $|\lambda_q|^2(\omega + k_p I_{\lambda_q}) = 0$, which holds if:

$$\omega = -k_p I_{\lambda_q}, \tag{3.6}$$

with $|\lambda_q| \neq 0$. Notice that (3.4) and (3.5) also imply that:

$$h = 1/(\gamma - k_p R_{\lambda_q}). \tag{3.7}$$

Multiplying (3.7) by (3.6), defining $\chi = h\omega$, and solving for $\gamma$ yield:

$$\gamma = k_p(R_{\lambda_q} - I_{\lambda_q}/\chi). \tag{3.8}$$

Moreover, from (3.5) we have that $\tan\left(h\omega - \angle\lambda_q\right) = 0$. Since $\chi = h\omega$, (3.8) is true if:

$$\chi = \angle\lambda_q \pm i\pi, \quad i = 1, 2, \ldots. \tag{3.9}$$

Recall that $k_p > 0$ and $h > 0$, then (3.2) follows from (3.8), denoting $\gamma = \gamma_q^i$ and $\chi = \chi_q^i$ and noticing that the polarity of $i$ in (3.9) must be the opposite of that of $I_{\lambda_q}$ in order to guarantee $\gamma_q^i > 0$. Finally, $h$ in (3.3) is equivalent to (3.7), and $k_r$ in (3.3) is obtained from (3.5). □

From this theorem, we remark that a maximum decay rate $\bar{\gamma}_q$ in the $q$-th factor is achieved when $\gamma_q^i$ is maximized. Clearly, $\bar{\gamma}_q = \gamma_q^1$ can be trivially proved from (3.2) by analyzing the variation of $\gamma_q^i$ with respect to $\chi_q^i$. That is, $d\gamma_q^i/d\chi_q^i = k_p I_{\lambda_q} \mathrm{sign}(I_{\lambda_q})/(\chi_q^i)^2 > 0$. Furthermore, the tuning for the $h$ and $k_r$ parameters obtained in Theorem 3.1.1 is identical for a pair of complex conjugate Laplacian eigenvalues. This allow us to study only the elements of $G_\lambda$ that correspond to the odd eigenvalues, namely $\lambda_q$, $q = 1, 3, \ldots, n_2$, on the first quadrant of $\mathbb{C}$.

### 3.1.2 Tuning of the PR protocol for right-most pole placement

We next prove that $\gamma_q^i$ in (3.2) is indeed associated with the real part of the rightmost root of $q$-th factor $f_{\lambda_q}$.

**Theorem 3.1.2.** *Let* $\lambda_q = |\lambda_q| \, \mathrm{e}^{j\angle\lambda_q} \in \mathbb{C}^+$ *with* $|\lambda_q| > 0$ *and* $\angle\lambda_q \in (0, \pi/2)$ *for* $q = 1, 3, \ldots, n_2$

*and let $\gamma_d > 0$ be a desired exponential decay rate. Then, the spectral abscissa of the $q$-th system $\dot{\zeta}_{\lambda_q}$ in (2.19) is placed at $-\gamma_d$ by tuning the gains of the PR protocol as*

$$(k_p, h, k_r) = \left( \frac{\gamma_d \chi_q^i}{R_{\lambda_q} \chi_q^i - I_{\lambda_q}},\ \frac{1}{\gamma_d - k_p R_{\lambda_q}},\ \frac{-\mathrm{e}^{-\gamma_d h}}{|\lambda_q|\, h \cos(-i\pi)} \right), \tag{3.10}$$

*where $\chi_q^i = \angle\lambda_q - i\pi$ and $i = 1, 2, \ldots$.*

*Proof.* First we show that Theorem 3.1.1 can be used to prescribe a desired maximum $\gamma_d$. To this end, solve $k_p$ from (3.2) and use $\gamma_q^i = \gamma_d$ into the result and into (3.3). Therefore, tuning formulas (3.10) allow us to attain a user-defined maximum $\gamma_d$. Next, we investigate whether the real part of the rightmost root of the $q$-th factor is placed at the desired position under (3.10). From Corollary 2.2.1, it is not difficult to see that the characteristic equation of the $q$-th system is $s + \lambda_q k_p - \lambda_q k_r \mathrm{e}^{-sh} = 0$, equivalently,

$$h(s + \lambda_q k_p)\, \mathrm{e}^{h(s+\lambda_q k_p)} = \lambda_q h k_r\, \mathrm{e}^{\lambda_q h k_p}. \tag{3.11}$$

Observe that $h\big(s + \lambda_q k_p\big) = W(\lambda_q h k_r\, \mathrm{e}^{\lambda_q h k_p})$ when (2.2) and (3.11) are compared. Here, $W(\diamond)$ denotes the Lambert W function we introduced in the preliminaries. Solving the above equation for $s$ yields:

$$s = h^{-1} W\big(\lambda_q h k_r\, \mathrm{e}^{\lambda_q h k_p}\big) - \lambda_q k_p. \tag{3.12}$$

With $(k_p, h, k_r)$ in (3.10) and $\lambda_q = R_{\lambda_q} + jI_{\lambda_q}$, the system's dominant root follows from (3.12) using the principal branch of the Lambert W function as:

$$s_{0,q} = h^{-1} W_0\big(-1\,\mathrm{e}^{-1}\big) + h^{-1} - \gamma_d + j\omega. \tag{3.13}$$

The proof is completed by noticing that $W_0\big(-1\,\mathrm{e}^{-1}\big) = -1$, hence, $\alpha_{\lambda_q} = -\gamma_d$. □

Notice that in the above proof, the designed characteristic root indeed adopts the dominant position on the complex plane within the infinite spectrum of $f_{\lambda_q}$. This means that Theorem 3.1.2 guarantees the $\gamma_d$-stability of the $q$-th factor. We next study how tuning (3.10) affects the stability of the remaining factors in $G_\lambda$.

### 3.1.3 Competing factors and stability interests in $G_\lambda$

Considering that the tuning (3.10) is implemented across every element $f_\lambda \in G_\lambda$, it is possible that the spectral abscissa $\alpha_{\lambda_{m_2}}$ arising from a factor $f_{\lambda_{m_2}}$, $m_2 \neq q$ may be larger. That is, the design based on system $q$ may give only sub-optimal results in another system $m_2$. In such cases, the spectral abscissa of the overall system will be governed by $\alpha_{\lambda_{m_2}}$, not by $\alpha_{\lambda_q}$. Our next result is concerned with this issue:

**Theorem 3.1.3.** *Let $\gamma_d > 0$ be given. Then, the set $G_\lambda$ is $\gamma_d$-stable by tuning the gains of the PR protocol as:*

$$(k_p, h, k_r) = \left( \frac{\gamma_d \chi_1^i}{\chi_1^i R_{\lambda_1} - I_{\lambda_1}},\ \frac{I_{\lambda_1} - \chi_1^i R_{\lambda_1}}{\gamma_d I_{\lambda_1}},\ \frac{-\mathrm{e}^{-\gamma_d h}}{|\lambda_1|\, h(-1)^i} \right), \tag{3.14}$$

*provided that the inequality*

$$F_{1,m_2}^i(\mathcal{G}) = \chi_1^i (R_{\lambda_{m_2}} - R_{\lambda_1}) + I_{\lambda_1}(R_{\mathcal{W}_{1,m_2}^i} + 1) < 0, \tag{3.15}$$

*holds for $m_2 = 3, 5, \ldots, n_2 - 1$ and some fixed $i \in \mathbb{Z}^+$, where $\chi_1^i = \angle\lambda_1 - i\pi$ and $R_{\mathcal{W}_{1,m_2}^i}$ is obtained from*

$$\mathcal{W}_{q,m_2}^i = R_{\mathcal{W}_{q,m_2}^i} + jI_{\mathcal{W}_{q,m_2}^i} = W_0\left( -1e^{-1} \frac{\lambda_{m_2}\, \mathrm{e}^{-\chi_q^i(\lambda_{m_2} - R_{\lambda_q})/I_{\lambda_q}}}{|\lambda_q| \cos(-i\pi)} \right), \tag{3.16}$$

*with $q = 1$.*

*Proof.* Consider two arbitrary rightmost roots $s_{0,q}$ and $s_{0,m_2}$, where $q \neq m_2$, associated respectively with the $q$-th and $m_2$-th subsystems of $\dot{\zeta}_\lambda \in G_\lambda$ with $\lambda_q$ and $\lambda_{m_2}$ on the first-quadrant of $\mathbb{C}$ without loss of generality. Here, we have a total of $(n_2 - 1)/2$ such eigenvalues, and $q, m_2 = 1, 3, \ldots, n_2$. We introduce the identity

$$\mathcal{S}_{q,m_2} = R_{\mathcal{S}_{q,m_2}} + jI_{\mathcal{S}_{q,m_2}} = s_{0,m_2} - s_{0,q}, \tag{3.17}$$

relating the rightmost roots. Then, if $\mathrm{sign}(R_{\mathcal{S}_{q,m_2}}) = -1$, we obtain that $\alpha_{\lambda_{m_2}} \leq \alpha_{\lambda_q}$. Applying Theorem 3.1.2 yields $\alpha_{\lambda_q} = -\gamma_d$. Further, the $m_2$-th and $q$-th subsystems are both $\gamma_d$-stable if and only if $\alpha_{\lambda_{m_2}} \leq \alpha_{\lambda_q} = -\gamma_d$ holds provided that $\gamma_d > 0$. Using the principal branch of the Lambert W function we have that (3.17) is given by

$$\mathcal{S}_{q,m_2} = h^{-1} W_0\left(\lambda_{m_2} h k_r\, \mathrm{e}^{\lambda_{m_2} h k_p}\right) - \lambda_{m_2} k_p - h^{-1} W_0\left(\lambda_q h k_r\, \mathrm{e}^{\lambda_q h k_p}\right) + \lambda_q k_p. \tag{3.18}$$

With $(h, k_p, k_r)$ in (3.10), the above can be rewritten as

$$\mathcal{S}_{q,m_2} = \frac{-\gamma_{d_q}}{\chi_q^i R_{\lambda_q} - I_{\lambda_q}} \left( \chi_q^i (R_{\lambda_{m_2}} - R_{\lambda_q}) + j\chi_q^i (I_{\lambda_{m_2}} - I_{\lambda_q}) + I_{\lambda_q}(R_{\mathcal{W}_{q,m_2}^i} + jI_{\mathcal{W}_{q,m_2}^i} + 1) \right), \tag{3.19}$$

where $R_{\mathcal{W}_{q,m_2}^i}$ and $I_{\mathcal{W}_{q,m_2}^i}$ are given by (3.16). Since $\chi_q^i < 0$ and $\gamma_{d_q}, R_{\lambda_q}, I_{\lambda_q} > 0$, then we have that $-\gamma_{d_q}/(\chi_q^i R_{\lambda_q} - I_{\lambda_q}) > 0$ holds. It follows from (3.19) that

$$\mathrm{sign}(R_{\mathcal{S}_{q,m_2}}) = \mathrm{sign}\left(\chi_q^i (R_{\lambda_{m_2}} - R_{\lambda_q}) + I_{\lambda_q}(R_{\mathcal{W}_{q,m_2}^i} + 1)\right) = \mathrm{sign}\left(F_{q,m_2}^i(\mathcal{G})\right). \tag{3.20}$$

Recognizing that $\text{sign}\big(F^i_{q,m_2}(\mathcal{G})\big)$ is influenced only by the topology of the graph-Laplacian $\mathcal{G}$ we can conclude that the very structure of the network determines whether or not $\gamma_d$-stability can be achieved by the proposed PR protocol within the $G_\lambda$ set. Furthermore, considering the numbering of the $\lambda$ eigenvalues represented by (2.9), one can make comparisons with respect to the first complex eigenvalue by setting $q = 1$ in $F^i_{q,m_2}(\mathcal{G})$ in (3.20), which is (3.15). Thus, guaranteeing that $\chi^i_1(R_{\lambda_{m_2}} - R_{\lambda_1}) < 0$ for all $m_2 \in \overline{1,n_2}$. Moreover, (3.14) follows from (3.10) with $q = 1$ and after some algebraic manipulations. Finally, if (3.15) holds for some $i \in \mathbb{Z}^+$ fixed, and an odd $m_2$ with $m_2 \neq q$, then $\text{sign}(R_{\mathcal{S}_{q,m_2}}) = -1$, ultimately guaranteeing the $\gamma_d$-stability of the $G_\lambda$ set. □

It is worthy of mention that the above theorem guarantees that $\max(\alpha_\lambda) = -\gamma_d$. The problem now is to determine how $(h, k_p, k_r)$ in (3.14) organizes the set of spectral abscissas $\alpha_\mu$. More precisely, we are interested in finding whether the $G_\mu$ set is $\gamma_d$-stable under this particular tuning. We also state the following remark.

**Remark 3.1.1.** *Notice that if (3.15) is true for a given positive $i$, it would also be true for larger $i$ values. In the rest of this manuscript, we shall restrict ourselves to the case where $i$ in (3.14) is an odd number, which in turn imply that the ratio $k_r/k_p$ is positive.*

## 3.2 Stability of the $G_\mu$ set

In general, the Laplacian matrix $L$ is allowed to have real and complex eigenvalues. As stated above, the question we wish to address here is: Could Theorem 3.1.3 be used to achieve $\gamma$-stability for $G_\lambda$ and $G_\mu$ concurrently? To answer this question, in this section we investigate how the tuning of the PR controller based on complex eigenvalues influences the spectral abscissas associated with the factors within $G_\mu$.

### 3.2.1 Contrasting the sets

We first show that the dominant spectral abscissa within the $G_\mu$ set is stable. We then use this information to propose a re-design of the PR consensus protocol.

**Theorem 3.2.1.** *Let $(h, k_p, k_r)$ be given as in (3.14), then $\max(\alpha_\mu) = \alpha_{\mu_1}$.*

*Proof.* Consider an arbitrary factor $f_{\mu_q} \in G_\mu$ associated with the real Laplacian eigenvalue $\mu_q > 0$. From Corollary 2.2.1, it is not difficult to see that $f_{\mu_q} = s + \mu_q k_p - \mu_q k_r \, \mathrm{e}^{-sh}$. Let the Laplace operator $s$ and the quasipolynomial $f_{\mu_q}$ be scaled by $\mu_q k_p$ and $1/(\mu_q k_p)$, respectively. We have that

$$f_{\mu_q}/(\mu_q k_p) = s + 1 - (k_r/k_p)\, \mathrm{e}^{-s\mu_q h k_p}. \tag{3.21}$$

Notice that the above transformation does not alter stability properties of the quasipolynomial. Since the triplet $(h, k_p, k_r)$ is fixed as per (3.14), it follows that the ratio $k_r/k_p$ and the product $hk_p$ are both constant. With this in mind, let us define $a = k_r/k_p$, $b = \mu_q h k_p$ and $f_b = f_{\mu_q}/(\mu_q k_p)$. Notice that $b > 0$ for every eigenvalue $\mu_q$ and as per Remark 3.1.1 $a > 0$. With these definitions, we obtain the non-dimensional representation of (3.21) as

$$f_b = s + 1 - a\,\mathrm{e}^{-sb}. \tag{3.22}$$

Using the principal branch of the Lambert W function, the rightmost root $s_0$ of $f_b$ is readily computed as

$$s_0 = b^{-1} W_0\big(ab\,\mathrm{e}^{b}\big) - 1. \tag{3.23}$$

We are interested on how the real part of $s_0$ behaves with respect to $b$. We further scale $s_0$ by $b$ and extract the real part of the result as

$$\alpha(b) = \mathsf{Re}\big(W_0(c)\big) - b. \tag{3.24}$$

where $c = ab\,\mathrm{e}^{b}$. Since $a > 0$ and $b > 0$, we have that $c > 0$. Differentiating the above with respect to $b$, we obtain

$$\frac{d\alpha(b)}{db} = \mathsf{Re}\left(\frac{dW_0(c)}{dc}\frac{dc}{db}\right) - 1 = \frac{1+b}{b}\mathsf{Re}\left(\frac{W_0(c)}{1+W_0(c)}\right) - 1. \tag{3.25}$$

Let $W_0(c) = R_w + jI_w$, with which the above can be rewritten as

$$\frac{d\alpha(b)}{db} = \frac{1+b}{b}\frac{(1+R_w)R_w + I_w^2}{(1+R_w)^2 + I_w^2} - 1. \tag{3.26}$$

We are interested in the sign of the above equality; i.e.,

$$G(b) = \mathrm{sign}\,\big(d\alpha(b)/db\big). \tag{3.27}$$

Since $W_0(z)$ is real for any $z > -1/\mathrm{e}$ and $c > 0$, it follows that $I_w = 0$:

$$\frac{d\alpha(b)}{db} = \frac{1+b}{b}\frac{R_w}{(1+R_w)} - 1 \tag{3.28}$$

Similarly, $W_0(z) > 0$ for any $z > 1$, hence $b(1+R_w) > 0$. Moreover $R_w = W_0(c)$, then we have that $G(b)$ is determined by:

$$G(b) = \mathsf{sign}\big((1+b)R_w - b(1+R_w)\big) = \mathsf{sign}\big(R_w - b\big) = \mathsf{sign}\big(W_0(c) - b\big). \tag{3.29}$$

Using the identity $z = W_0(z\,\mathrm{e}^{z})$, we have that:

$$G(b) = \mathsf{sign}\big(W_0(ab\,\mathrm{e}^{b}) - W_0(b\,\mathrm{e}^{b})\big) = \mathsf{sign}(ab\,\mathrm{e}^{b} - b\,\mathrm{e}^{b}) = \mathsf{sign}(a-1) < 0, \tag{3.30}$$

follows from the definition of $k_p$ and $k_r$ in (3.14). That is, the spectral abscissa monotonically decreases with $b$. The proof is completed by noticing that $\lim_{b\to 0}\alpha(b)=0$. □

From Theorem 3.4, we know that $\alpha_{\mu_1}$ is the largest spectral abscissa in $G_\mu$. Therefore, it suffices to prove the $\gamma_d$-stability of $\alpha_{\mu_1}$ to guarantee the $\gamma_d$-stability of the whole set $G_\mu$. To begin with, observe from (3.30) that $a-1<0$, hence:

$$0<a<1,$$

or equivalently, $k_r<k_p$. Multiplying both sides of this inequality by a positive term $h\mu_1 \mathrm{e}^{(h\mu_1 k_p)}$ we have that $h\mu_1 k_r \mathrm{e}^{(h\mu_1 k_p)} < h\mu_1 k_p \mathrm{e}^{(h\mu_1 k_p)}$. Notice also from the above that the following holds:

$$W_0\left(h\mu_1 k_r \mathrm{e}^{(h\mu_1 k_p)}\right) < W_0\left(h\mu_1 k_p \mathrm{e}^{(h\mu_1 k_p)}\right),$$

where $W_0$ is the principal branch of the Lambert W function. Using once more the identity $z=W_0(z\mathrm{e}^z)$ and rearranging the terms we obtain:

$$\frac{1}{h}W_0\left(h\mu_1 k_r \mathrm{e}^{(h\mu_1 k_p)}\right)-\mu_1 k_p<0. \tag{3.31}$$

This inequality will be useful to prove the next result:

**Corollary 3.2.1.** *Let $(h,k_p,k_r)$ be given as in (3.14), then the set $G_\mu$ is stable.*

*Proof.* The factor $f_{\mu_1}$ associated with the first eigenvalue of the $G_\mu$ group is readily obtained as $s+\mu_1 k_p-\mu_1 k_r \mathrm{e}^{\gamma_d h-sh}=0$. Multiplying both sides of the above equation by $h\mathrm{e}^{h\mu_1 k_p}$, we have that:

$$(sh+h\mu_1 k_p)\mathrm{e}^{(sh+h\mu_1 k_p)} = h\mu_1 k_r \mathrm{e}^{h\mu_1 k_p}. \tag{3.32}$$

It follows from the Lambert W function that

$$W(h\mu_1 k_r \mathrm{e}^{h\mu_1 k_p}) = sh+h\mu_1 k_p.$$

Solving the above equation for $s$ and using the principal branch of the Lambert W function, we find that the spectral abscissa is given by

$$\alpha_{\mu_1} = \mathrm{Re}\left\{\frac{1}{h}W_0\left(h\mu_1 k_r \mathrm{e}^{h\mu_1 k_p}\right)-\mu_1 k_p\right\}. \tag{3.33}$$

Since $h\mu_1 k_r \mathrm{e}^{h\mu_1 k_p}>0$, we have that $W_0\left(h\mu_1 k_r \mathrm{e}^{h\mu_1 k_p}\right)$ is pure real, see Figure 2.4. The proof is concluded by noticing from (3.31) that $\alpha_{\mu_1}<0$. □

### 3.2.2 Tuning of the PR protocol for $\gamma_d$-stability

At this point, the design of the PR controller is able to provide stability. Recall however that the main objective here is to achieve fast consensus, which is related with the placement of the spectral abscissa of the overall system. On the one hand, as concluded in the previous section, the position of $\alpha_{\mu_1}$ on the complex plane ensures the stability of the $G_\mu$ set. On the other hand, to establish $\gamma_d$-stability of $G_\mu$ it is necessary that $\alpha_{\mu_1} \leq -\gamma_d$. In other words, if $\gamma_d + \alpha_{\mu_1} \leq 0$ we have that $G_\lambda$ and $G_\mu$ are both $\gamma_d$-stable. Whenever the above condition does not hold, a re-design of the PR protocol would guarantee $\gamma_d$-stability [13].

**Corollary 3.2.2.** *Let $\gamma_d > 0$ be a desired exponential decay and let $(k_p, h, k_r)$ be given as in (3.14). If $\gamma_d + \alpha_{\mu_1} \leq 0$, then the MAS defined by* (1.1) *in closed-loop with* (1.2) *is $\gamma_d$-stable. If $\gamma_d + \alpha_{\mu_1} > 0$ then, tuning the gains of the PR protocol as*

$$(k_p', h', k_r') = \left( -\frac{\gamma_d}{\alpha_{\mu_1}} \frac{\gamma_d \chi_1^i}{\chi_1^i R_{\lambda_1} - I_{\lambda_1}},\ -\frac{\alpha_{\mu_1}}{\gamma_d} \frac{I_{\lambda_1} - \chi_1^i R_{\lambda_1}}{\gamma_d I_{\lambda_1}},\ \frac{-\mathrm{e}^{\gamma_d^2/\alpha_{\mu_1} h'}}{|\lambda_1| h' (-1)^i} \right), \tag{3.34}$$

*guarantees that* (1.1)-(1.2) *is $\gamma_d$-stable.*

*Proof.* The first part of the proof, where $\gamma_d + \alpha_{\mu_1} \leq 0$, is trivial by noting that $(k_p, h, k_r)$ are tuned as per Theorem 3.1.3. For the second part of the proof, where $\gamma_d + \alpha_{\mu_1} > 0$, we first introduce the following change of variable:

$$\gamma_d \longrightarrow -\left( \frac{\gamma_d}{\alpha_{\mu_1}} \right) \gamma_d.$$

Then, under the above shift, the set of parameters in (3.14) is mapped into (3.34). Notice that this transformed parameters can be written in terms of $(k_p, h, k_r)$ as follows:

$$(k_p', h', k_r') = (k_p, h, k_r) \Big|_{\gamma_d \longrightarrow -\left(\frac{\gamma_d}{\alpha_{\mu_1}}\right)\gamma_d}. \tag{3.35}$$

According to Corollary 3.2.1, this new set of parameters $(k_p', h', k_r')$ will place the spectral abscissa of (1.1)-(1.2) at a new position $\alpha_{\mu_1}'$, namely:

$$\alpha_{\mu_1}' = \frac{1}{h} \frac{-\gamma_d}{\alpha_{\mu 1}} W_0 \left( \frac{\alpha_{\mu 1}}{-\gamma_d} h \mu_1 \frac{-\gamma_d}{\alpha_{\mu 1}} k_r \mathrm{e}^{h\mu_1 k_p} \right) - \frac{-\gamma_d}{\alpha_{\mu 1}} \mu_1 k_p.$$

Notice that this new placement for the spectral abscissa is also given in terms of the former $\alpha_{\mu_1}$ in (3.33). Then, after some algebraic manipulations, the above reduces to

$$\alpha_{\mu_1}' = -\frac{\gamma_d}{\alpha_{\mu_1}} \left[ \frac{1}{h} W_0 \left( h\mu_1 k_r \mathrm{e}^{h\mu_1 k_p} \right) - \mu_1 k_p \right] = -\frac{\gamma_d}{\alpha_{\mu_1}} \alpha_{\mu_1} = -\gamma_d.$$

We conclude that the re-design process places the dominant spectral abscissa $\alpha'_{\mu_1}$ at $-\gamma_d$, guaranteeing the $\gamma_d$-stability of the overall network. □

Since we are substituting $\gamma_d$ for an even larger value, the roots of the $G_\lambda$ set will be pushed further to the left on the complex plane and the spectral abscissa of $G_\lambda$ is now placed at $-(\gamma_d/\alpha_{\mu_1})\gamma_d$, we obviate further analysis on it.

# Chapter 4

# Simulation and experimental results

In this chapter, we test the tuning approach developed in Chapter 3 via simulations and experiments. First, considering a network with six agents, a numerical simulation is performed in MATLAB® using `dde23` function. The goal here is to show how consensus reaching can be accelerated by an appropriate tuning of the proposed distributed PR protocol. Next, as a preliminary step to the experimental validation of our tuning approach, we make sure that the control algorithm studied here performs reasonably well on Georgia Tech Robotarium simulator —a MAS simulator coded in MATLAB®—. Finally, with the above simulation results, we implement the PR protocol (1.2) in the Robotarium experimental platform demonstrating its validity in a real-world application.

## 4.1 Numerical results

The proposed methodology is tested first via a numerical example. Since the developments are analytic, the design technique must guarantee the exact placement of the spectral abscissa. We study fast consensus in a network with six agents; here, the communication infrastructure is described by the direct graph $\mathcal{G}$ depicted in Figure 4.1. For simplicity, agents' coupling strengths are taken to be homogeneous and binary; i.e, the entries of the adjacency matrix are either $1$ or $0$. With $\mathcal{G}$ being connected, the graph Laplacian matrix is defined as

$$L = \begin{pmatrix} 3 & -1 & 0 & -1 & -1 & 0 \\ 0 & 3 & -1 & -1 & 0 & -1 \\ -1 & 0 & 2 & 0 & 0 & -1 \\ -1 & -1 & -1 & 5 & -1 & -1 \\ -1 & -1 & -1 & 0 & 3 & 0 \\ -1 & 0 & 0 & 0 & 0 & 1 \end{pmatrix}, \tag{4.1}$$

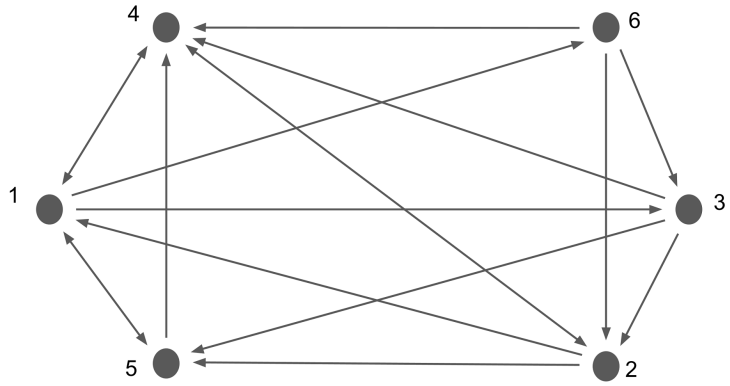


Figure 4.1: Topology of the six-agent network $(n = 6)$ described by a directed graph $\mathcal{G}$.

which has a $\nu = 0$ eigenvalue, and the rest of its eigenvalues are either complex or real, namely,

$$\lambda = \{2.8203 - j0.9030, 2.8203 + j0.9030\} \quad \text{and} \quad \mu = \{2, 4, 5.3593\}.$$

Having computed the Laplacian eigenvalues, with $\gamma_d = 1.925$[1] , we find from Theorem 3.1.3 the initial tuning

$$(k_p, h, k_r) = \left(0.6132,\ \ 5.113,\ \ 3.5033 \times 10^{-6}\right)$$

for the parameters of the PR protocol (1.2). With these numerical values, the distribution of the rightmost roots of the MAS are next computed using QPmR [30] as depicted in Figure 4.2 (left panel). The characteristic roots associated with real and complex eigenvalues are shown with dots and asterisks, respectively, whereas the root associated with the zero eigenvalue is drawn with an $\times$ marker. The dashed vertical line is placed at $-\gamma_d$. From the figure, it is clear that the rightmost root associated with the real Laplacian eigenvalues is dominant. In other words,

$$\gamma_d + \alpha_{\mu_1} > 0,$$

and hence a re-design of the controller parameters is in order. Following Corollary 3.2.2 we obtain

$$(k_p', h', k_r') = \left(0.9654,\ \ 3.2484,\ \ 5.5152 \times 10^{-6}\right),$$

with which the distribution of the rightmost roots of the MAS is re-computed as in Fig-

[1] It is worth mentioning that $\gamma_d$ is chosen here to generate a realizable delay $h$ in Robotarium, namely, a multiple of the inherent delay fixed at a value of 0.033s.

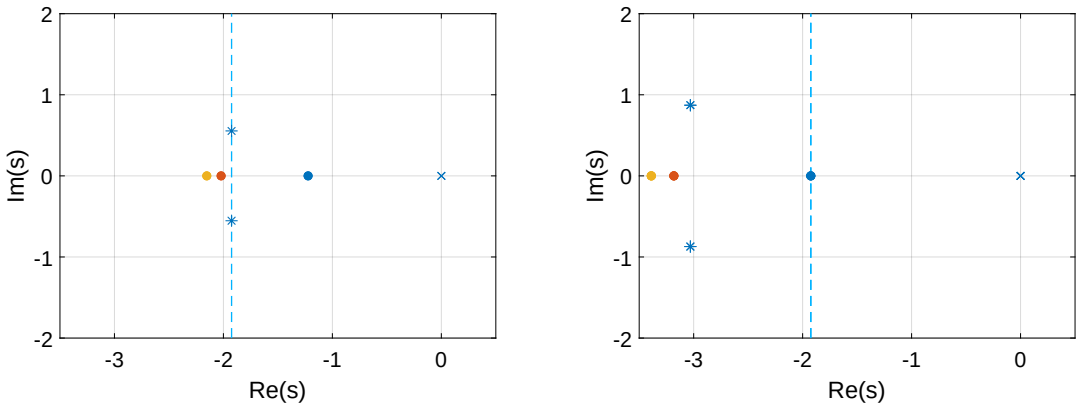


Figure 4.2: Six-agent network subject to the PR protocol (1.2). The characteristic roots associated with real and complex eigenvalues are depicted with dots and asterisks, respectively. Desired decay rate $\gamma_d = 1.925$. (Left panel) Spectrum distribution using Theorem 3.1.3. (Right panel) Spectrum distribution using Corollary 3.2.2.

ure 4.2 (right panel). Notice that the dominant spectral abscissa $\alpha_{\mu_1}$ is placed at the desired locus $\alpha_{\mu_1} = -\gamma_d$ as guaranteed by Corollary 3.2.2, ultimately establishing the $\gamma_d$-stability of the overall MAS.

Figure 4.3 shows the time simulations in MATLAB® using the embedded function `dde23` for several desired decay rates; i.e.,

$$\gamma_d \in \{1.925, 10.415, 35.03, 48.17\},$$

and considering the continuous initial function $x(\theta) = \sigma$ with $\theta \in [-h, 0]$ and $\sigma \in \mathbb{R}^n$. From the figure, one can conclude that increasing $\gamma_d$ can be understood as a spectral shifting that reduces the time needed for the agents to reach an agreement. To estimate the converge rate we measure the settling time $t_{set}$, defined by a $0.5\%$ settling rule on the total displacement

$$\|x\| = \left[\sum_{i=1}^{n} x_i^2(t)\right]^{1/2}, \tag{4.2}$$

of all the agents. Table 4.1 summarizes the result. Clearly, as $\gamma_d$ increases, $t_{set}$ decreases.

Table 4.1: Settling time based on a $0.5\%$ rule

| $\gamma_d$ | $h$ | $k_p$ | $k_r$ | $t_{set}$ |
|---|---|---|---|---|
| 1.925 | 3.24 | 0.9654 | $5.5152 \times 10^{-6}$ | 1.005 |
| 10.415 | 0.6004 | 5.2230 | $2.983 \times 10^{-5}$ | 0.185 |
| 35.03 | 0.1785 | 17.5672 | $1.0036 \times 10^{-4}$ | 0.0553 |
| 48.17 | 0.1298 | 24.1567 | $1.38 \times 10^{-4}$ | 0.0402 |

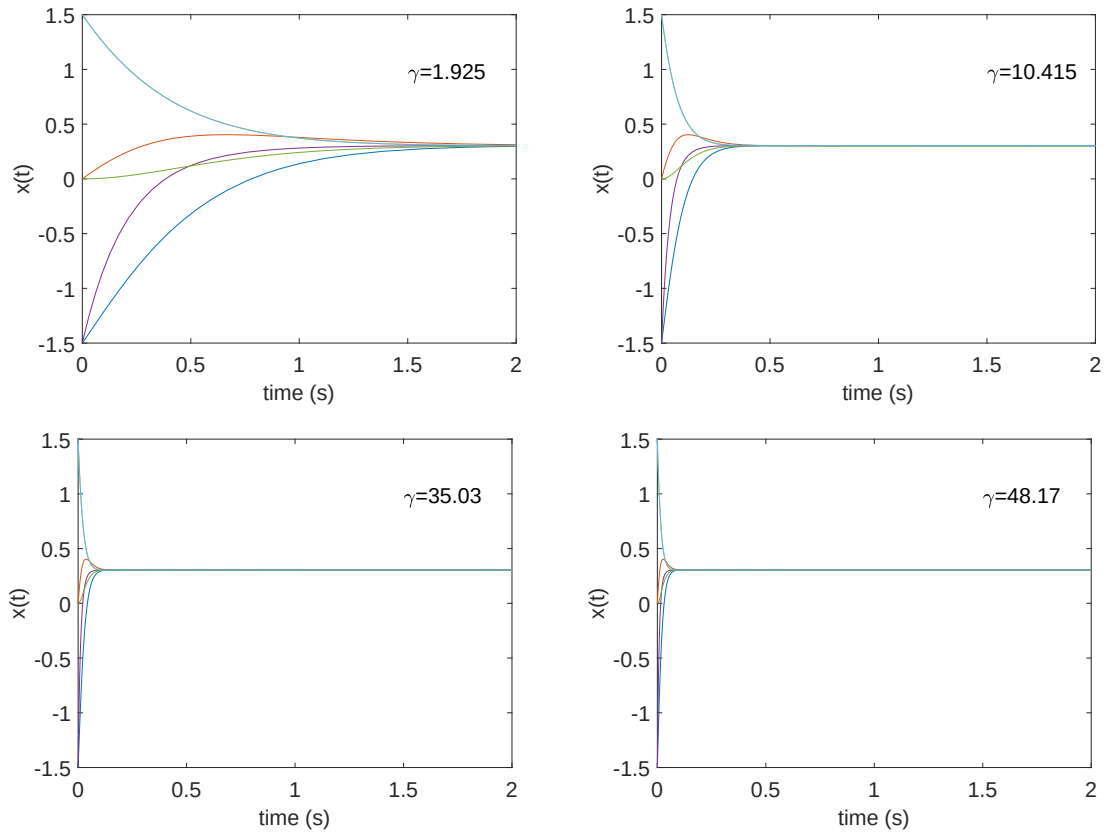


Figure 4.3: Trajectories of the agents based on time simulations for different desired decay rates $\gamma_d \in \{1.925, 10.415, 35.03, 48.17\}$.

## 4.2 Robotarium

Georgia Tech's Robotarium [31] is a research project that provides remote access to a swarm robotics research platform. Robotarium is focused on providing the means to test algorithms on real hardware. Since the main focus of this thesis is to develop the theory associated with fast consensus reaching, Robotarium provides a valuable tool to demonstrate and test our findings. In addition, a virtual environment coded in MATLAB® is also available with which preliminary testing of algorithms may be performed.

Robotarium agents are nonholonomic differential-drive robots and their dynamics are modelled with an unicycle model:

$$\dot{\vec{x}} = \begin{bmatrix} \cos(\theta) & 0 \\ \sin(\theta) & 0 \\ 0 & 1 \end{bmatrix} \begin{bmatrix} v \\ \omega \end{bmatrix},$$

where $\vec{x} = [x, y, \theta]^T$ represent the position and orientation of the robot, and $v$ and $\omega$ are the linear and angular velocities, respectively. In many applications is convenient to map

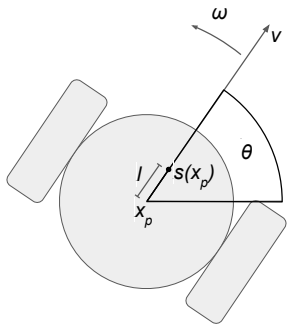


Figure 4.4: Representation of a differential-drive robot.

the unicycle model to a single-integrator representation, as is the case of this research project. For completeness, here we summarize the single-integrator mapping given in [31]. Figure 4.4 represents a differential-drive robot and the parameters used to describe its motion. Consider a full-state vector $\vec{x} = [x, y, \theta]^T$ and a global position vector $\vec{x}_p = [x, y]^T$. Next, a point perpendicular to the wheel axis at a distance $l$ is defined as:

$$s(\vec{x}) = \vec{x}_p + l \begin{pmatrix} \cos(\theta) \\ \sin(\theta) \end{pmatrix}, \quad l > 0.$$

Notice that $[v, \omega]^T$ represents the unicycle control inputs of linear and angular velocities. Although the global position vector $\vec{x}_p = [x, y]^T$ is constrained by the nonholonomic construction of the vehicle[2], the velocity of the $s(\vec{x})$ point is not. Using a near-identity diffeomorphism, the single-integrator dynamics of $s(\vec{x})$ are found, given unicycle velocity control inputs. Thus, taking the time derivative of $s(\vec{x})$ yields:

$$\dot{s}(\vec{x}) = \dot{\vec{x}}_p + l\dot{\theta} \begin{bmatrix} -\sin(\theta) \\ \cos(\theta) \end{bmatrix}.$$

Substituting the unicycle dynamic model for $\vec{x}_p$ and $\theta$ gives:

$$\dot{s}(\vec{x}) = R_l(\theta) \begin{bmatrix} v \\ \omega \end{bmatrix} \quad \text{where} \quad R_l(\theta) = \begin{bmatrix} \cos(\theta) & -l\sin(\theta) \\ \sin(\theta) & l\cos(\theta) \end{bmatrix}.$$

For $l \neq 0$, **the input generated by our single-integrator-based algorithm** can be approximated as $\dot{s}(\vec{x})$ and mapped to an input for the differential-drive robot as:

$$\begin{bmatrix} v \\ \omega \end{bmatrix} = R_l^{-1}(\theta)\dot{s}(\vec{x}).$$

[2] In the case of unicycle differential-drive robots, this constrain means that the vehicle cannot move sideways. This characteristic is not compatible with the single integrator dynamics so the mapping is positioned slightly off-center to allow holonomic movement.

### 4.2.1 Simulations

In what follows, we use the Robotarium simulator to test the PR consensus protocol (1.2). It is worth mentioning that consensus was successfully reached considering the tuning formulas obtained in Corollary 3.2.2, however, a clear relation between larger values of $\gamma_d$ and shorter settling times was not found at first. Further inspection of the results demonstrated that the physical constrains —given by the real capabilities of the robots, coded within the simulator— did not allow for this relation to be measured. With this in mind, a modification of the simulator was performed with which faster velocities on the agent's wheels were enabled[3]. This modification resulted in a correlation between shorter settling times and larger values of $\gamma_d$, thus validating the proposed approach. Additional clarity in the simulation results can be obtained by omitting the collision avoidance barrier implemented in the original code. This allows agents to occupy the same physical space, giving a clear picture of consensus reaching. Yet, the construction of the agents[4] force them to rotate around the consensus state indefinitely, as shown here or in the url: `https://www.youtube.com/watch?v=tahqQTlnfXE`. This circular motion translates into oscillations in the total displacement of the agents as measured by (4.2). Nevertheless, as this phenomena is unrelated to the protocol performance, is disregarded when estimating settling times.

#### Small-scale network

Considering a PR network with six agents with an underlying graph as the one shown in Figure 4.1, for several values of $\gamma_d$, Table 4.2 summarizes the delay values $h$ obtained with (3.14), the corresponding consensus settling times and the associated total control efforts ($TCE$) defined as

$$TCE = \int_0^{t_{set}} \|u\| dt, \tag{4.3}$$

where $\|u\| = \left[\sum_{i=1}^{n} u_i^2(t)\right]^{1/2}$.

An increase in control effort is naturally associated with larger values of $\gamma_d$, as expected. An example of this simulation tests is presented in Figure 4.7. In the figure, agents start in a predetermined rectangular formation and deploy the PR protocol to eventually reach consensus autonomously as time increases.

[3] The maximum linear velocity of the simulated agents was increased from $0.2$ m/s to $0.5$ m/s. We consider this modification to be reasonable since a nominal speed of $0.5$ m/s could be feasibly implemented in this type of systems without compromising the safety of the robots.

[4] Agents are built as two wheeled differential drive robots so their movement is not omnidirectional. If they get close enough to the consensus point, their construction induces them to rotate around it

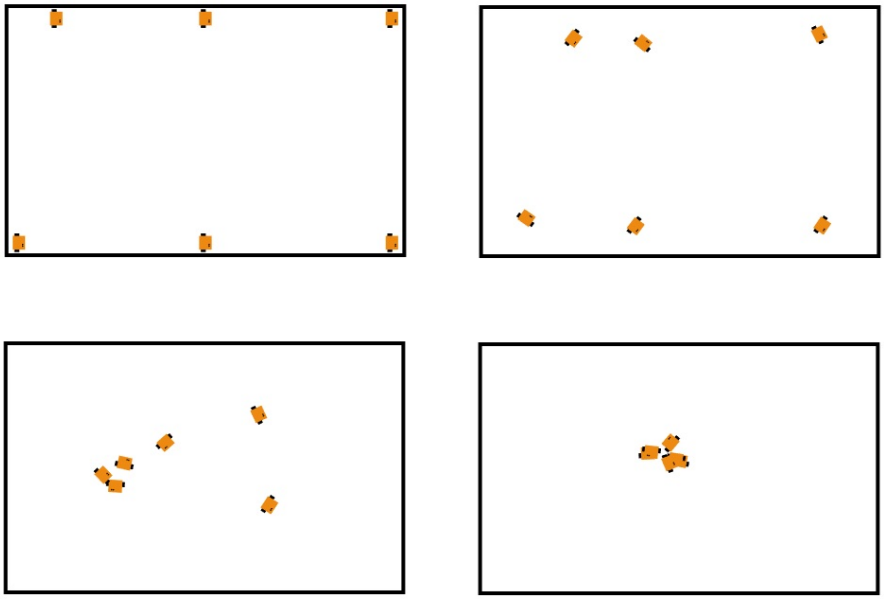

Figure 4.5: Screenshots of the simulation for a six-agent PR network. Time elapses from top to bottom and left to right: agents start in a rectangular formation to next deploy the PR protocol reaching consensus in position about the center of the test bed.

Table 4.2: $TCE$ and $t_{set}$ based on a $0.5\%$ rule.

| $\gamma_d$ | $h(s)$ | $t_{set}(s)$ | $TCE$ |
|---|---|---|---|
| 0.9474 | 6.60 | 9.2070 | 22.4771 |
| 1.1843 | 5.28 | 5.4780 | 29.2651 |
| 1.8949 | 3.30 | 3.993 | 50.2183 |
| 3.7899 | 1.65 | 3.86 | 110.79 |
| 5.121 | 1.221 | 3.729 | 147.51 |

**Scalability**

Next, to investigate the effect of driving a larger number of agents, we simulate a twenty-agent MAS subject to the PR protocol (1.2) and the tuning formulas in (3.14). The MAS communication infrastructure is abstracted in the directed graph depicted in Figure 4.6. Since the graph is connected, the Laplacian matrix has a $\nu = 0$ eigenvalue and the rest of eigenvalues are obtained as

$$\begin{aligned}\lambda = \{&1.426 \pm j0.7751, 1.7643 \pm j1.3288, 1.8084 \pm j0.9039,\\ &2.2036 \pm j0.8919, 2.50 \pm j0.866, 2.7363 \pm j0.3214, 3.1889 \pm j0.1429\},\\ \mu = \{&0.7695, 1, 1.1881, 2, 3.7873\},\end{aligned}$$

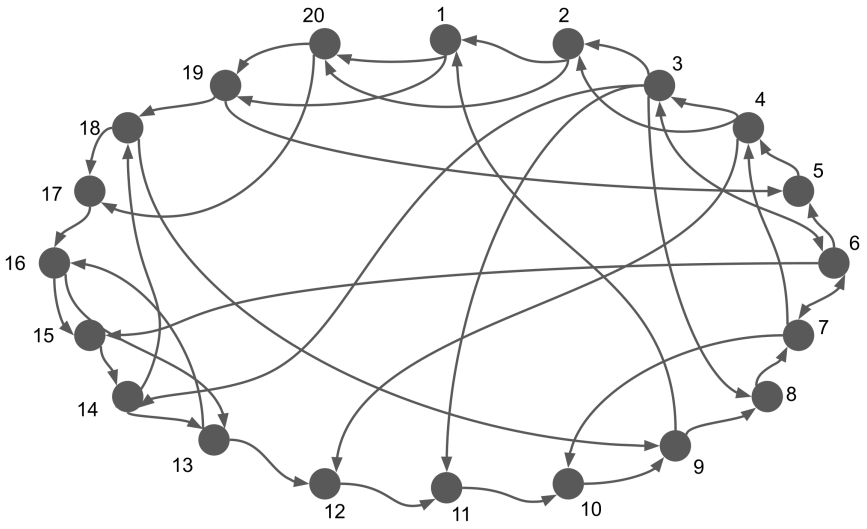


Figure 4.6: A representation of the directed graph that governs the MAS communication.

Choosing a desired value for $\gamma_d = 1.5797$, we first compute the initial parameters

$$(h, k_p, k_r) = (3.7120,\ \ 0.9189,\ \ 0.0005),$$

following Theorem 3.1.3. With the above, we find that

$$\gamma_d + \alpha_{\mu_1} > 0$$

for this particular system, hence a re-design of the PR protocol is in order. After adjusting the parameters $(h, k_p, k_r)$ as per Corollary 3.2.2 we obtain that

$$(h', k_p', k_r') = (1.65,\ \ 2.0672,\ \ 0.0011), \tag{4.4}$$

and $\gamma_d$-stability is finally guaranteed as further verified by computing the spectrum distribution of the MAS at hand. The evolution of the system is obtained in the Robotarium simulation environment disregarding collision avoidance barriers as discussed above. The simulation resulted in a settling time $t_{set} = 7.953$ s and a total control effort $TCE = 34.14$, both in the same order of magnitude than those in the six-agent examples. It is worth mentioning that any additional computations are not needed whenever the number of agents increases. In other words, the approach is scalable and the number of agents becomes irrelevant in the tuning process developed in this thesis.

### 4.2.2 Experiments

Finally, we test our developments on Georgia Tech Robotarium test bed considering first a six-agent network.

**Small-scale network**

For the actual Robotarium implementation, we make use of the previously studied topology depicted in Figure 4.1. The individual agents are placed in a rectangular grid at first and then, the proposed PR consensus algorithm is performed for $\gamma = 29.58$. For this particular system we already know that the rightmost root associated with the real Laplacian eigenvalues is dominant. After re-designing the controller parameters with Corollary 3.2.2, we obtain

$$(k_p', h', k_r') = (14.834, \quad 0.2114, \quad 8.4747 \times 10^{-5}).$$

The result is illustrated in Figure 4.7 with four frames of the Robotarium execution, showing the agents' movements first from an arbitrary starting position, then to a predefined rectangular grid and finally carrying out the consensus protocol. The full experiment was captured in video and can be accessed at here or in the next url: `https://youtu.be/821-tHmNdtk`

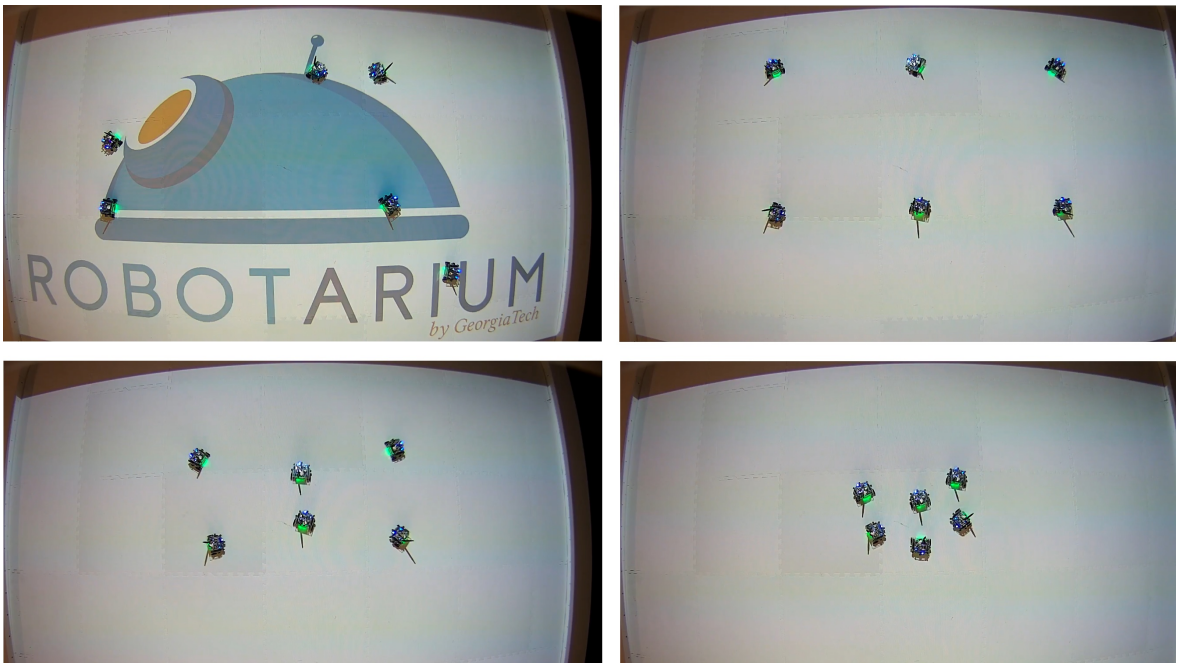


Figure 4.7: Robotarium agents performing the consensus protocol. Time elapses from top to bottom and left to right: Agents finding an arbitrary initial position. Getting to a fixed rectangular formation. Performing the consensus protocol. Agents reaching consensus in position.

# Chapter 5

# Conclusions and future work

The thesis presents analytical formulas to tune the parameters $(h, k_p, k_r)$ of a distributed PR consensus protocol for a class of single-integrator MAS with the main objective of creating a desired (maximum) exponential decay rate for the solutions of the closed-loop system. The developments exposed throughout this manuscript revolves around the idea of designing the dominant modes of the collective dynamics. These dominant modes are further associated with fast consensus reaching as evidenced by means of numerical and experimental data.

To our best knowledge, for the class of MAS studied here, an analytically-derived PR tuning technique has not been proposed in previous research. In this sense, the ideas developed in the present manuscript complement the state of the art. Moreover, since the results are analytic, we believe that the tuning process is accessible enough, from an algorithmic point of view, to be used as a ready-to-use tool. Although the results are specialized for MAS with single-integrator agents, our developments could be utilized as the baseline toward analyzing more complex problems, where inter-agent communication is described by directed graphs and characterized by complex conjugate and pure real Laplacian eigenvalues.

Fast consensus has become an important measure of performance in MAS. However, in some situations, the realization of delay may be constrained by the very structure of the system. In such cases, from a practical point of view, it would be more convenient to choose an priory realizable delay value to then compute the corresponding attainable decay rate $\gamma$ and the corresponding set of gain values. The above observation was necessary in the experimental stage of this work. More precisely, in the Robotarium platform, a specific time lag is inherent to the communication of the agents' state. Hence, tuning of the PR protocol was performed with the intention of generating a realizable artificial delay, which is a multiple of the communication lag.

Questions about how scalability and different topologies impact fast consensus are to be investigated in the future to further complement this research. In theory, it is always possible to extend the consensus protocol to an arbitrary number of agents. Yet, it is a known fact that implementation becomes problematic as the number of agents grow. Also, there is a considerable amount of research [21, 17, 14] on how fast consensus can benefit from adequate graph topology selection. For this project, however, it would be enough to generate strongly connected graphs in a random way to be our experimental topology. In spite of the obtained analytical results, the nature of the analysis still requires some computations. In Theorem 3.1.3, for example, it is necessary to check inequality (3.15), which may be challenging in a large-scale setting. However, the inequality is usually validated at the first or second iteration, which sheds light into the possible existence of a more general and accurate theory. On the other hand, at the end of Chapter 3, we state the need of verifying whether $\alpha_{\mu_1}$ is smaller or equal to $-\gamma_d$. In case $\alpha_{\mu_1} > -\gamma_d$, a re-tuning process needs to be performed. We acknowledge that a simpler, more direct procedure is desirable, which is left to future investigations.

# Bibliography


[1] Farshid Maghami Asl and Galip Ulsoy. Analysis of a system of linear delay differential equations. *Journal of Dynamic Systems, Measurement, and Control*, 125(2):215–223, 2003.

[2] Albert-László Barabási. *Network science*, volume 371. The Royal Society Publishing, 2013.

[3] Vivek Borkar and Pravin Varaiya. Asymptotic agreement in distributed estimation. *IEEE transactions on automatic control*, 27(3):650–655, 1982.

[4] Dimitri Breda. On characteristic roots and stability charts of delay differential equations. *International journal of robust and nonlinear control*, 22(8):892–917, 2012.

[5] Robert M Corless, Gaston H Gonnet, David EG Hare, David J Jeffrey, and Donald E Knuth. On the lambertw function. *Advances in Computational mathematics*, 5(1):329–359, 1996.

[6] Marcio De Queiroz, Xiaoyu Cai, and Matthew Feemster. *Formation Control of Multi-agent Systems: A Graph Rigidity Approach*. John Wiley & Sons, 2019.

[7] Richard C Dorf and Robert H Bishop. *Modern control systems*. Pearson Prentice Hall, 2008.

[8] Veysel Gazi and Kevin M Passino. *Swarm stability and optimization*. Springer Science & Business Media, 2011.

[9] Veysel Gazi and Kevin M Passino. *Swarm stability and optimization*. Springer Science & Business Media, 2011.

[10] Jack K Hale and Sjoerd M Verduyn Lunel. *Introduction to functional differential equations*, volume 99. Springer Science & Business Media, 2013.

[11] Roger A Horn and Charles R Johnson. *Matrix analysis*. Cambridge university press,

2012.

[12] Irena Jadlovská. Application of lambert w function in oscillation theory. *Acta Electrotechnica et Informatica*, 14(1):9–17, Sep 2014.

[13] Min Hyong Koh, Adrián Ramírez, and Rifat Sipahi. Single-delay proportional-retarded (pr) protocols for fast consensus in a multi-agent system. *IFAC-PapersOnLine*, 51(14):31–36, 2018.

[14] Min Hyong Koh and Rifat Sipahi. Achieving fast consensus by edge elimination in a class of consensus dynamics with large delays. *2016 American Control Conference (ACC)*, pages 5364–5369, 2016.

[15] Wim Michiels and Silviu-Iulian Niculescu. *Stability and stabilization of time-delay systems: an eigenvalue-based approach*. SIAM, 2007.

[16] Bogdan Nica. *A brief introduction to spectral graph theory*. 2016.

[17] Reza Olfati-Saber. Ultrafast consensus in small-world networks. *Proceedings of the 2005, American Control Conference, 2005.*, pages 2371–2378, 2005.

[18] Reza Olfati-Saber, Alex Fax, and Richard M Murray. Consensus and cooperation in networked multi-agent systems. *Proceedings of the IEEE*, 95(1):215–233, 2007.

[19] Reza Olfati-Saber and Richard M Murray. Consensus protocols for networks of dynamic agents. 2003.

[20] Reza Olfati-Saber and Richard M Murray. Consensus problems in networks of agents with switching topology and time-delays. *IEEE Transactions on automatic control*, 49(9):1520–1533, 2004.

[21] Wei Qiao, Fatihcan M Atay, and Rifat Sipahi. Graph laplacian design for fast consensus of a lti system with heterogeneous agent couplings and homogeneous inter-agent delays. American Society of Mechanical Engineers Digital Collection, 2013.

[22] Adrián Ramírez and Rifat Sipahi. Multiple intentional delays can facilitate fast consensus and noise reduction in a multiagent system. *IEEE transactions on cybernetics*, 49(4):1224–1235, 2018.

[23] Adrián Ramírez and Rifat Sipahi. Single-delay and multiple-delay proportional-retarded (pr) protocols for fast consensus in a large-scale network. *IEEE Transactions on Automatic Control*, 64(5):2142–2149, 2018.

[24] Adrian Ramirez, Rifat Sipahi, Sabine Mondié, and Ruben Garrido. An analytical

approach to tuning of delay-based controllers for lti-siso systems. *SIAM Journal on Control and Optimization*, 55(1):397–412, 2017.

[25] Adrián Ramírez, Rifat Sipahi, Sabine Mondié, and Rubén Garrido. Fast consensus in a large-scale multi-agent system with directed graphs using time-delayed measurements. *Philosophical Transactions of the Royal Society A*, 377(2153):20180130, 2019.

[26] Wei Ren and Randal W Beard. *Distributed consensus in multi-vehicle cooperative control*, volume 27. Springer, 2008.

[27] Andrew R Teel and Laurent Praly. A smooth lyapunov function from a class-kl estimate involving two positive semidefinite functions. *ESAIM: Control, Optimisation and Calculus of Variations*, 5:313–367, 2000.

[28] John Tsitsiklis and Michael Athans. On the complexity of decentralized decision making and detection problems. *IEEE Transactions on Automatic Control*, 30(5):440–446, 1985.

[29] John Tsitsiklis, Dimitri Bertsekas, and Michael Athans. Distributed asynchronous deterministic and stochastic gradient optimization algorithms. *IEEE transactions on automatic control*, 31(9):803–812, 1986.

[30] Tomas Vyhlidal and Pavel Zítek. Mapping based algorithm for large-scale computation of quasi-polynomial zeros. *IEEE Transactions on Automatic Control*, 54(1):171–177, 2009.

[31] Sean Wilson, Paul Glotfelter, Li Wang, Siddharth Mayya, Gennaro Notomista, Mark Mote, and Magnus Egerstedt. The robotarium: Globally impactful opportunities, challenges, and lessons learned in remote-access, distributed control of multirobot systems. *IEEE Control Systems Magazine*, 40(1):26–44, 2020.

[32] Lin Xiao and Stephen Boyd. Fast linear iterations for distributed averaging. *Systems & Control Letters*, 53(1):65–78, 2004.

[33] Sun Yi, Patrick W Nelson, and Galip Ulsoy. *Time-delay systems: analysis and control using the Lambert W function*. World Scientific, 2010.

[34] Sun Yi, Patrick W Nelson, and Galip Ulsoy. *Time-delay systems: analysis and control using the Lambert W function*. World Scientific, 2010.